Article:
Jamaludin, N.A., Thurston, L.M., Witek, K.J. et al. (2019) Efficient isolation, biophysical characterisation and molecular composition of extracellular vesicles secreted by primary and immortalised cells of reproductive origin. Theriogenology, 135. pp. 121-137. ISSN: 0093-691X

https://doi.org/10.1016/j.theriogenology.2019.06.002

Accepted Manuscript

Efficient isolation, biophysical characterisation and molecular composition of extracellular vesicles secreted by primary and immortalised cells of reproductive origin.

Nurul Akmal Jamaludin, Lisa Marie Thurston, Krzysztof Jan Witek, Albany Meikle, Shaghayegh Basatvat, Sarah Elliott, Stuart Hunt, Aneta Andronowska, Alireza Fazeli

PII:	S0093-691X(19)30223-7
DOI:	10.1016/j.theriogenology.2019.06.002
Reference:	THE 15037
To appear in:	*Theriogenology*
Received Date:	14 February 2019
Accepted Date:	04 June 2019

Please cite this article as: Nurul Akmal Jamaludin, Lisa Marie Thurston, Krzysztof Jan Witek, Albany Meikle, Shaghayegh Basatvat, Sarah Elliott, Stuart Hunt, Aneta Andronowska, Alireza Fazeli, Efficient isolation, biophysical characterisation and molecular composition of extracellular vesicles secreted by primary and immortalised cells of reproductive origin., *Theriogenology* (2019), doi: 10.1016/j.theriogenology.2019.06.002

Title:

Efficient isolation, biophysical characterisation and molecular composition of extracellular vesicles secreted by primary and immortalised cells of reproductive origin.

Nurul Akmal Jamaludin[1], Lisa Marie Thurston[1,2], Krzysztof Jan Witek[3], Albany Meikle[1], Shaghayegh Basatvat[1], Sarah Elliott[1], Stuart Hunt[4], Aneta Andronowska[3], Alireza Fazeli[1,5]*

1. Academic Unit of Reproductive and Development Medicine, Department of Oncology and Metabolism, University of Sheffield, Sheffield S10 2SF, UK
2. Department of Comparative Biomedical Sciences, Royal Veterinary College, University of London, London NWI 0TU, UK
3. Institute of the Animal Reproduction and Food Research of the Polish Academy of Sciences, 10-748 Olsztyn, Poland
4. The School of Clinical Dentistry, University of Sheffield, Sheffield S10 2TA, UK
5. Department of Pathophysiology, University of Tartu, Tartu, Estonia

Corresponding author:

*Professor Alireza Fazeli

Chair of Reproductive and Developmental Medicine

Academic Unit of Reproductive and Development Medicine, University of Sheffield,

Level 4, The Jessop Wing, Tree Root Walk, Sheffield, S10 2SF, UK

a.fazeli@sheffield.ac.uk

Declaration of Interest:

The authors declare that they have no declarations of interest.

Author email addresses:

Nurul Akmal Jamaludin (nakmaljamaludin@gmail.com); Lisa Marie Thurston (lthurston@rvc.ac.uk); Krzysztof Jan Witek (k.witek@pan.olsztyn.pl); Albany Meikle (Albany.meikle@gmail.com); Shaghayegh Basatvat (s.basatvat@sheffield.ac.uk); Sarah Elliott (s.elliott@sheffield.ac.uk); Stuart Hunt (s.hunt@sheffield.ac.uk); Aneta Andronowska (a.andronowska@pan.olsztyn.pl); Alireza Fazeli (a.fazeli@sheffield.ac.uk).

Abstract

Effective communication between the maternal reproductive tract, gametes and the pre-implantation embryo is essential for the successful establishment of pregnancy. Recent studies have recognised extracellular vesicles (EVs) as potent vehicles for intercellular communication, potentially via their transport of microRNAs (miRNAs). The aim of the current investigation was to determine the size, concentration and electrical surface properties (zeta potential) of EVs secreted by; (1) primary cultures of porcine oviductal epithelial cells (POECs) from the isthmus and ampullary regions of the female reproductive tract; (2) Ishikawa and RL95-2 human endometrial epithelial cell line cultures; and (3) the non-reproductive epithelial cell line HEK293T. In addition, this study investigated whether EVs secreted by POECs contained miRNAs. All cell types were cultured in EV-depleted medium for 24 or 48 hours. EVs were successfully isolated from conditioned culture media using size exclusion chromatography. Nanoparticle tracking analysis (NTA) was performed to evaluate EV size, concentration and zeta potential. QRT-PCR was performed to quantify the expression of candidate miRNAs (miR-103, let-7a, miR-19a, miR-203, miR-126, miR-19b, RNU44, miR-92, miR-196a, miR-326 and miR-23a). NTA confirmed the presence of EVs with diameters of 50-150 nm in all cell types. EV size distribution was significantly different between cell types after 24 and 48 hours of cell culture and the concentration of EVs secreted by POECs and Ishikawa cells was also time dependent. The distribution of EVs with specific electrokinetic potential measurements varied between cell types, indicating that EVs of differing cellular origin have varied membrane components. In addition, EVs secreted by POECs exhibited significantly different time dependant changes in zeta potential. QRT-PCR confirmed the presence of miR-103, let-7a, miR-19a, miR-203, miR-126, and miR-19b in EVs secreted by POECs (C_T ≥29). Bioinformatics analysis suggests that these miRNAs are involved in cell proliferation, innate immune responses, apoptosis and cellular migration. In conclusion, reproductive epithelial cells secrete distinct populations of EVs containing miRNAs, which potentially act in

intercellular communication in order to modulate the periconception events leading to successful establishment of pregnancy.

Keywords:

Extracelluar vesicle, oviductal epithelial, MicroRNA, exosome.

1. Introduction

Beneficial communication between the female reproductive tract and the gametes is essential for the successful establishment of fertilisation [1]. In order for spermatozoa to fertilise an oocyte in the oviduct, they must first travel through the complex structures of the female reproductive tract, where they undergo biochemical modification and sperm selection [2]. Recent studies have sought to determine the complex molecular interactions between spermatozoa and the cells of the female reproductive tract, investigating mechanisms of gamete storage in the oviduct [2-3], the control of gamete maturation [4] and the selection of specific populations of spermatozoa for fertilisation [5]. While significant advances have been made in the understanding of the resultant effects of exposure of gametes to oviductal fluid and/or the binding of spermatozoa to oviductal epithelial cells, specific details regarding intercellular communication remain elusive [6-10].

It is widely accepted that extracellular vesicles (EVs) are powerful vehicles for intercellular communication in a wide variety of physiological systems [11-14]. The term EV refers to a diverse classification of vesicles secreted by the cell and includes microvesicles (50-1000 nm in diameter and of plasma membrane origin), exosomes (50-150 nm in diameter, originating from endosomal cellular compartments) and apoptotic bodies (100-2000nm in diameter) [14-18]. EVs are composed of a lipid bilayer containing transmembrane proteins and enclosing soluble proteins, DNA, and RNA (including microRNAs) [12, 15, 19-20]. Once secreted by their cell of origin, it is thought that recipient cells are able to target and bind EVs via their surface proteins thus mediating communication between cell types [21].

In the mammalian reproductive system, EVs have been identified in semen [22], uterine fluid [23-24], oviductal fluid [25-26] and follicular fluid [27], where they have been reported to be involved in gametogenesis, fertilization, embryogenesis and embryo development [24, 28-29]. Data from our research group have demonstrated that EVs are secreted by both uterine and oviductal epithelial cells of the porcine female reproductive tract [30]. Moreover, in humans, endometrial epithelial cells have been shown to secrete EVs, which carry extracellular matrix metalloprotease inducer (EMMPRIN) for the production of matrix metalloproteinase in uterine stromal fibroblast cells, an essential component of endometrial remodelling during the menstrual cycle and during embryo implantation [23, 31-32]. In rodents, oviductal epithelial cell EVs are known to deliver essential fertility modulating proteins, including plasma membrane Ca^{2+} regulatory ATPase 4 (PMCA4), to the spermatozoa in order to modulate sperm storage, capacitation and acrosome reaction [25]. More recently, Alminana *et al*. [33] have shown that EVs secreted by bovine oviductal epithelial cells *in vivo* and *in vitro,* contain proteins known to be involved in sperm-oocyte binding, fertilisation and embryo development. Since the discovery of EVs on the apical surfaces of oviductal and endometrial epithelial cells, and also in oviductal and uterine fluid, research into the roles of EVs within the reproductive system have given some clues as to the mechanisms that might be used to achieve successful intercellular communication.

It is thought that EVs might facilitate their potent effects on intercellular communication via their transport and delivery of microRNAs (miRNAs) [13]. MiRNAs are known to influence both the protein translocation of genes, and the non-coding RNA mediated signalling cascades that regulate differential splicing events and thus impact cellular processes [34]. As the interaction of gametes with the maternal reproductive tract is known to be accompanied by the upregulation of proteins in maternal tract epithelia, a potential mechanism of regulation for these interactions might be via EV-mediated miRNA delivery [35-37]. Recently, we have obtained data indicating that spermatozoa secrete EVs that interact with oviductal epithelial

cells when in sperm-oviduct co-cultures [38]. MiRNAs have previously been detected in spermatozoa and it is interesting to note that sperm miRNA complement differs between fertile and infertile men [39]. Further clarification of the miRNA content of EVs secreted by oviductal epithelial cells, and their potential modification of both the gametes and the female tract itself, would have significant implications for the targeting of assisted reproductive technologies.

To date, EVs have been characterised based on their size and concentration, and their expression of specific biomarkers including the Tetraspanins [40-42]. In addition, scanning electron microscopy (SEM) has proved to be a useful tool for the demonstration of the presence of EVs isolated from cell culture medium, urine, plasma and breastmilk, however, this technique is not quantitative and provides no detailed information regarding the size distribution or the total number of EVs within a given sample [42]. Here, we describe a novel method for establishing the characteristics of individual extracellular vesicles in real time using nanoparticle tracking analysis (NTA) by ZetaView® (Particle Metrix, Germany). NTA uses laser scattering microscopy to detect the random movement of individual EVs within a solution. The ZetaView® NTA software uses video tracking to measure the rate of EV Brownian motion to calculate the diffusion coefficient and thus determine particle size and concentration [16, 43]. In addition to determining EV size parameters, ZetaView® NTA is able to measure the electrokinetic potential, or zeta potential, of the interfacial region between the EV surface and its aqueous environment [44-45]. This zeta potential measurement is able to provide us with important information regarding the stability of the colloid system, since it measures the attraction or repulsion between particles, by providing an indication of the magnitude of their electrostatic charge [44, 46-47]. However, perhaps more importantly, the zeta potential measurement reflects the surface charge of the EV membrane [48]. As plasma membrane composition is known to influence cellular surface charge, and thus zeta potential [49], it is not unreasonable to assume that the content of the EV membrane might also be reflected in its

zeta potential providing us with a mechanism for classifying EVs based on their membrane content [48].

Given the increased interest in the potential of EVs as facilitators of intercellular communication and the application of this new technology across all physiological systems, it is imperative that we develop rigorous *in vitro* systems with which to study the content, action and effects of EVs secreted by different cell types. Moreover, the identification of EV miRNAs and the clarification of their function in mediating intercellular communication, will enhance our understanding of how cells are able to influence the physiology of their surrounding environment. This is of particular importance for our understanding of reproductive physiology, where defining the type and function of EVs that are produced by different reproductive cells will provide important insights into the mechanisms influencing fertilisation by natural conception and assisted reproductive technologies. Therefore, the aim of this present study was to develop an *in vitro* system for the production, isolation and characterisation of EVs secreted by porcine oviductal epithelial cells (POECs) in primary culture, human endometrial epithelial cell lines (Ishikawa and RL95-2), and the non-reproductive human embryonic kidney epithelial cell line HEK293T. In addition, we will determine whether POECs secrete EVs that contain bioactive molecules including EV-specific protein biomarkers and miRNAs.

2. Materials and methods

2.1. Cell culture

2.1.1. Primary porcine oviductal epithelial cell (POEC) cultures.

Oviducts were obtained from reproductively immature gilts immediately after slaughter at a local abattoir (N.Bramall and Sons Ltd., UK). The oviducts were dissected on site from supporting mesentery, ovaries and uterine horns and were transported back to the laboratory on ice in Dulbecco's Phosphate Buffered Saline (DPBS) with calcium and magnesium supplemented with a 2% antibiotic antimycotic mix (10,000 units/ml penicillin, 10 mg/mL streptomycin and 25 µg/ml amphotericin) (Sigma-Aldrich®, Poole, UK). In the laboratory, the oviducts and oviductal lumens were washed three times with DPBS (Sigma-Aldrich®) supplemented with the 2% antibiotic antimycotic mix. Oviducts were then tied with a cotton ligature at the ampullary end, filled with 0.25% collagenase solution (Sigma-Aldrich®) and closed at the utero tubal junction (UTJ) with an additional cotton ligature. Oviducts were incubated in Hank's Balance Salt Solution (Sigma-Aldrich®) in a humidified atmosphere of 5% CO_2 in air, at 39^0C for 90 minutes. Thereafter, the oviducts were cut at the ampullary end and the luminal content, containing the POECs, was harvested by squeezing the lumen content. For investigations comparing POECs from different regions of the oviduct, the oviduct was bisected at the isthmus-ampullary junction and porcine ampulla epithelial cells (PAECs) and porcine isthmus epithelial cells (PIECs) were recovered from the ampullary and isthmic regions of the oviduct, respectively. POECs, PAECs or PIECs were placed into F-12 Ham Nutrient Mixture medium supplemented with 10% (v/v) foetal bovine serum (FBS; Sigma-Aldrich®), 1% (v/v) antibiotic antimycotic mix (Sigma-Aldrich®). The harvested POECs, PAECs or PIECs, were washed 3 times with complete medium by centrifugation at 300 x *g* at room temperature for 5 minutes. Cell pellets were treated with cold distilled water to remove red blood cells and were then washed once more by centrifugation at 300 x *g* at room

temperature for 5 minutes. POECs, PAECs or PIECs, were seeded in T75 flasks (1 x 10^6 cells per flask) (Greiner, Frickenhausen, Germany) and cultured in F-12 Ham Nutrient Mixture medium supplemented with 10% (v/v) FBS (Sigma-Aldrich®) in a humidified atmosphere of 5% CO_2 in air, at 39^0C. Culture medium was refreshed every 48 hours. After 4-5 days in culture, all cells had reached confluency. At confluency, POECs, PAECs and PIECs were harvested using trypsin-EDTA solution (Sigma-Aldrich®) and pelleted by centrifugation at 300 x *g* for 4 minutes before resuspension in culture media.

In order to isolate EVs, POECs, PAECs and PIECs (3 x 10^6 cells or 3 x T75 flasks where each flask contained 1 x 10^6 cells) were grown in F-12 Ham Nutrient Mixture medium supplemented with 10% (v/v) FBS. At 40% confluency, the medium was replaced with F-12 medium supplemented with 10% EV-depleted FBS and 1% (v/v) antibiotic antimycotic (Sigma-Aldrich®). Conditioned medium containing POEC-EVs was collected 24 hours and 48 hours after the culture medium was changed to an EV-depleted FBS media. Conditioned medium containing PAEC-EVs or PIEC-EVs was collected 48 hours after the culture medium was changed to an EV-depleted FBS media. All the experiments were performed using 3 biological replicates (independent porcine POEC, PAEC or PIEC cultures produced from porcine oviducts collected on different days) and 3 technical replicates (independent cell culture flasks).

2.1.1.1. Preparation of EV-depleted FBS

EV-depleted FBS was prepared by ultracentrifugation of FBS (Sigma-Aldrich®) at 100,000 x *g* overnight at 4°C (Beckman-Coulter, Optima™ LE-80K ultracentrifuge, type 45 Ti rotor). The resulting supernatant was filtered through a 0.22 µm filter. Following ultracentrifugation and filtration, the concentration of EVs in the resultant EV-depleted FBS was determined by NTA.

NTA was performed using the PMX 110 ZetaView® (Particle Metrix, Meerbusch, Germany), with ZetaView® sensitivity and shutter parameters set at 85 and 1/70 seconds respectively. To assess the efficiency of this method for FBS EV depletion, 3 different batches of EV-depleted FBS (biological replicates) were analysed with 3 technical assessments being carried out on each batch. However, all cell culture experiments reported in this manuscript were conducted using a single batch of EV-depleted FBS in order to standardise the effects of any serum-derived growth factors and/or biomolecules on cell proliferation and EV production.

2.1.2. Immortalised cell line cultures

Human endometrial adenosquamous carcinoma Ishikawa cells (Sigma-Aldrich®), human endometrial adenosquamous carcinoma RL95-2 cells (American Type Culture Collection, ATCC; Virginia, USA) and human embryonic kidney epithelial HEK293T cells (ATCC) were utilised in these investigations. Ishikawa cells were cultured in Minimum Essential Medium Eagle (Sigma-Aldrich®) supplemented with 10% (v/v) FBS and 1% L-Glutamine (Sigma-Aldrich®). RL95-2 cells were cultured in Dulbecco's Modified Eagle's Medium Nutrient Mixture F-12 (Sigma-Aldrich) supplemented with 10% (v/v) FBS, 1% L-Glutamine and 0.125% insulin (Gibco, ThermoFisher Scientific, Paisley, UK). HEK293T cells were cultured in Roswell Park Memorial Institute 1640 (RPMI-1640) medium (Sigma-Aldrich®) supplemented with 10% (v/v) FBS, 1% L-Glutamine (Sigma-Aldrich®) and 1% Minimum Essential Medium (MEM; Sigma-Aldrich®). For all human cell lines, 3 T75 flasks, where each flask contained 1 x 10^6 cells, were seeded and cultured in a humidified atmosphere of 5% CO_2 in air, at 37°C. Once the cell lines reached 40% confluency, medium was removed and replaced with the respective fresh culture medium supplemented with 10% EV-depleted FBS. Conditioned medium containing EVs, was collected after 24 hours and 48 hours of cell culture.

2.2. Extracellular vesicle isolation

2.2.1. Removal of cells and cell debris from conditioned media

Conditioned media containing EVs released from cell lines and primary cultures was centrifuged at 300 x *g* for 10 minutes at 4°C and the epithelial cell pellet discarded. The supernatant was centrifuged at 2000 x *g* for 10 minutes at 4°C and the pellet containing dead cells discarded. Finally, the remaining supernatant was centrifuged at 10,000 x *g* for 30 minutes at 4°C to pellet cellular debris. The final supernatant was concentrated using a Vivaspin 20 concentration tube (GE Healthcare, Buckinghamshire, UK) (100,000 Da molecular weight cut off) using a centrifugation force of 2500 x *g* at 4°C, until 0.5ml of concentrated conditioned media remained.

2.2.2. Size exclusion chromatography (SEC)

SEC was performed to isolate EVs from free proteins in the conditioned culture media. Fourteen millilitres of Sepharose CL-2B suspended in 20% ethanol (GE Healthcare, Uppsala, Sweden) was added to an Econo-Pac chromatography column (Bio-Rad, Hercules, USA) and allowed to settle until the ethanol had separated from the agarose beads. An upper bed support was placed into the column at a depth of 10 ml and the separated ethanol layer was allowed to elute from the column. DPBS (Sigma-Aldrich®) supplemented with 0.03% Tween-20 (Sigma-Aldrich®) (PBS+Tween) was passed through the column twice to wash any remaining ethanol from the Sepharose beads. Concentrated conditioned media containing EVs secreted by cell lines and primary cultures was added to the SEC column and simultaneously the collection of the elution was initiated. For each sample of concentrated EV conditioned media, a total of 20 fractions were collected from the SEC column, each containing a volume of 0.5 ml. After the total volume of concentrated EV conditioned media had passed through the upper bed support, 10 ml of PBS+Tween was added to the SEC column, in order to create a pressure for elution.

2.2.3. Bicinchoninic acid (BCA) assay

To determine the relative presence of protein in each of the POEC-EV SEC fractions, protein content was measured using the BCA assay. Bovine serum albumin (BSA) protein standards (Sigma-Aldrich®) were prepared with PBS+0.03% Tween (Sigma-Aldrich®), at final concentrations of 0, 0.2, 0.4, 0.6, 0.8, 1.0 and 2 µg/µl. Ten microlitres of each POEC-EV SEC fraction and the protein standards were placed into individual wells of a 96-well plate (Greiner Bio-One, Gloustershire, UK) in duplicate. Protein standards were used to evaluate any potential variation in measurements between plates. A 200 µl copper sulphate solution (Sigma-Aldrich®) with BCA solution (Sigma-Aldrich®) in a 1:50 ratio was added to each well and the plate was incubated at 37°C for 30 minutes. Absorbance was determined using a Multiscan EX microplate reader (MTX Labsystems, Bradenton, USA) at a wavelength of 570 nm and analysed using Ascent Software for Multiscan. A calibration curve of protein standard concentration versus absorption was produced and the protein concentration of each POEC-EV SEC fraction was calculated.

2.2.4. Sodium dodecyl sulphate (SDS) polyacrylamide gel electrophoresis

In order to visualise the relative presence of protein in each POEC-EV SEC fraction, protein content was profiled using polyacrylamide gel electrophoresis. Fifteen microliters of each POEC-EV SEC fraction was mixed with 15 µl of 2-fold concentrated reducing sample buffer with β-mercaptoethanol (5%; Bio-Rad, Watford, UK) and incubated at 95°C for 7 min. Then, 30 µl of each sample and 5 µl of Precision plus protein™ standard (Bio-Rad) was loaded onto a 12% SDS-PAGE polyacrylamide gel (National diagnostics, USA) and electrophoresis was performed for 90 min at 110 V. After that, gels were stained with Coomassie blue R-250 (Sigma-Aldrich®) for 1 hour at room temperature and then washed with destaining solution several times until the background became clear.

2.3. Western blot analysis of extracellular vesicles in EV-conditioned media using CD63 and CD9 protein markers

The presence of EVs in the POEC SEC fractions was confirmed by western blot analysis using the EV protein biomarkers CD63 and CD9. Six fractions containing the highest concentration of POEC-EVs (fractions 7 to 12) were pooled and centrifuged at 100 000 x *g* for 1 hour at 4ºC. The pellet was resuspend in radioimmunoprecipitation assay (RIPA) lysis buffer containing protease inhibitors (Thermo Fisher Scientific, Rockford, USA). Protein concentration was determined using the BCA assay method as previously described. Protein was resolved on 12% SDS-polyacrylamide gels (National diagnostics), transferred onto polyvinylidene fluoride (PVDF) membranes (Thermo Fisher Scientific), and blocked with 5% (w/v) non-fat milk powder suspended in TRIS-buffered saline with tween-20 (TBS-T; Sigma-Aldrich®). Protein blots were subsequently probed with a CD63 primary antibody (rabbit polyclonal antibody; Santa Cruz Biotechnology, Dallas, USA) or a CD9 primary antibody (mouse monoclonal antibody; Bio-Rad) at 1:200 dilution in 5% non-fat milk/TBS-T solution at 4ºC overnight. Blots were washed for 5 minutes in TBS-T four times and then incubated in secondary antibody, polyclonal goat anti-rabbit immunoglobulin/horseradish peroxidase (HRP) (Dako, Denmark) or polyclonal goat anti-mouse immunoglobulin/HRP (Thermo Fisher Scientific) for CD63 or CD9 respectively, at 1:2000 dilution at 4°C overnight. The PVDF membrane was then washed again with TBS-T three times for 10 minutes each. Pierce enhanced chemiluminescence (ECL) Western Blotting Substrate (Thermo Fisher Scientific; reagents A and B combined at a 1:1 ratio), was applied to the PVDF membrane for a few seconds to facilitate development. The blot was sandwiched between plastic and exposed to 5” x 7” CL-Xposure™ film (Thermo Fisher Scientific) in an x-ray cassette (Kodak, New York, USA) for between 5 to 20 minutes. The film was developed and fixed using a Compact X4 automatic x-ray film processor (Xograph,Gloucestershire, UK). All western blotting experiments were performed in triplicate.

2.4. Nanoparticle tracking analysis (NTA)

2.4.1. EV size and concentration measurement

Following SEC, POEC-EVs in each of 20 column fractions were measured by NTA to quantify EV size distribution and concentration. For PAEC-EVs, PIEC-EVs and cell line derived EVs, EV concentration and size distribution was determined in SEC fractions 5 to 15, as these fractions had previously been identified as containing a high EV concentration and low contaminating protein content. NTA was performed using the PMX 110 ZetaView® (Particle Metrix, Meerbusch, Germany). The Brownian motion of each EV was visualised by a laser light scattering method and tracked over time to calculate particle size using the Stokes-Einstein equation to determine the translational diffusion constant. All NTA measurements were performed with a ZetaView® sensitivity of 85, a shutter value of 70 (corresponding to an exposure time of 15 ms) and a frame rate of 30 frames per second. Column fractions were diluted between 1:20 and 1:200 in filtered distilled water to ensure that the concentration of EVs in each sample was optimal for ZetaView assessment (final concentration of 2.5×10^7 EVs per ml equates to 150 detected particles by the ZetaView®). In all experiments, three biological replicates and 3 technical assessments were carried out.

2.4.2. EV zeta potential measurement

Following SEC, POEC-EVs, PAEC-EVs, PIEC-EVs and cell line derived EVs were measured by NTA to quantify EV electrokinetic potential, or zeta potential (ζ). In all experiments, EVs from SEC fractions 5 to 15 were pooled for zeta potential analysis. Prior to measurement, the pooled fractions were diluted 1:100 in 1% PBS plus 0.03% Tween to ensure that the concentration of EVs in each sample was optimal for ZetaView assessment. EV zeta potential was measured using the PMX 110 ZetaView® (Particle Metrix). ZetaView® sensitivity was set at 85, shutter value at 70 (corresponding to an exposure time of 15 ms) and frame rate at 30 frames per second. For the zeta potential measurement, solution conductivity was determined

to be low (below 2 mS/m), and as such, continuous mode was chosen. A low conductivity solution contains less ions and thus there are no issues with electro-osmosis factors influencing electrokinetic potential measurements. For all samples, pH was measured using an IQ150 pH meter (Spectrum Technologies, Inc. USA) and if required, pH was adjusted to 6.9 with 1M HCl. All experiments were carried out on 3 biological replicates with 4 technical replicates.

2.5. Extracellular vesicle microRNA content analysis

In order to partially characterise the miRNA content of POEC-EVs, quantitative real time-PCR (QRT-PCR) analysis was carried out.

2.5.1. RNA extraction from extracellular vesicles

For RNA extraction, 400 µl aliquots from each of POEC-EV SEC fractions 7-12 were combined and added to a Vivaspin6 (GE Healthcare, Buckinghamshire, UK) concentration column (100,000 Da molecular weight cut off), and centrifuged at 2500 x *g* until 100 µl of a concentrated sample containing EVs remained.

2.5.1.1. Tri-Reagent extraction

RNA isolation from POEC-EVs was performed using the TRI Reagent® manufacturer's protocol (Sigma-Aldrich®). One millilitre of TRI Reagent was added to 100 µl of concentrated POEC-EVs. The EV lysate was homogenised by pipetting up and down several times. The homogenous lysate was transferred into a new tube and incubated for 5 minutes at room temperature to ensure the complete dissociation of membrane protein complexes. Then, 100 µl of 1-Bromo-3-chloropropane was added to the EV homogenate and the mixture was shaken vigorously for 15 seconds. After incubation at room temperature for 15 minutes, the sample was centrifuged for 15 minutes at 12,000 x *g* at 4 ºC resulting the production of 3 phases; a

red organic phase (protein), an interphase (DNA), and a colourless upper aqueous phase (RNA). The colourless aqueous phase was carefully transferred to a new tube and 500 µl of 2-propanol was added. The sample was then incubated at room temperature for 10 minutes. Subsequently, a centrifugation step was performed at 12,000 x *g* for 10 minutes at 4 ºC. Next, the supernatant was carefully removed from the tube and the pellet was washed by adding 1 ml 75 % Ethanol and centrifuged at 12,000 x *g* for 5 minutes at 4 ºC. The Ethanol phase was removed and the pellet was air dried for 5 minutes. Finally, the RNA was eluted with 50 µl RNAse-free water (Sigma-Aldrich®) and stored at -80 °C.

2.5.1.2. miRCURY RNA isolation kit

RNA was extracted from concentrated POEC-EV samples using a miRCURY RNA isolation kit (Exiqon, Woburn, USA) according to the manufacturer's instructions. In brief, the concentrated POEC-EV sample was lysed using the lysate buffer provided with the kit and 100% ethanol was added to the sample. The lysate was washed three times using the provided wash solution, using centrifugation. Elution buffer (provided) was added to the sample and used to elute RNA by centrifugation. The RNA was treated with RNase-Free DNase Set (Qiagen, USA) to avoid DNA contamination and was stored at -80 °C.

2.5.2. RNA detection

RNA quality, yield and size was measured using capillary electrophoresis (Agilent 2100 G2938B Model B Bioanalyzer; Agilent Technologies, Santa Clara, USA). Prior to analysis, RNAs were prepared with the Aqilent small RNA kit (Agilent Technologies) according to the manufacturer's protocol.

2.5.3. microRNA Expression Analysis

Quantification of miRNA expression was performed using the TaqMan miRNA Assay. Quantification using this assay is carried out using a two-step RT-PCR. First, complementary DNA (cDNA) is reverse transcribed from total RNA samples using Megaplex Primers Pool A

from the TaqMan miRNA Reverse Transcription Kit (Applied Biosystems, Foster City, USA). Second, the TaqMan miRNA Assay together with TaqMan Universal PCR Master Mix was used to amplify the PCR product from cDNA samples.

2.5.3.1. Reverse transcription reaction

A reverse transcription reaction was performed using the TaqMan miRNA Reverse Transcription Kit (Applied Biosystems) with Megaplex Primers Pool A according to the manufacturer's instructions. Briefly, for each 4.5 µl reaction, the RT master mix comprised 0.8 µl Megaplex™ RT Primers (10X), 0.2 µl dNTPs with dTTP (100mM), 1.5 µl MultiScribe™ Reverse Transcriptase (50 U/µL), 0.8 µl 10X RT Buffer, 0.9 µl $MgCl_2$ (25mM), 0.1 µl RNase Inhibitor (20U/µL) and 0.2 µl Nuclease-free water. Three microlitres of RNA template was added to the RT master mix, mixed gently and incubated on ice for 5 minutes. The reverse transcription reaction thermal-cycling conditions consisted of 40 cycles with a profile of 2 minutes at 16°C, 1 minute at 42 °C and 1 second at 50 °C, followed by 5 minutes at 85 °C.

2.5.3.2. Quantitative Real time-PCR (qRT-PCR)

Quantitative RT-PCR reactions were performed using the TaqMan miRNA Assay together with the TaqMan 2X Universal PCR master Mix No AmpErase UNG. All qRT-PCR reactions were performed in triplicate with every 20 µl reaction comprised of 1 µl TaqMan miRNA Assay (20X), 1.33 µl product from RT Reaction, 10 µl TaqMan 2X Universal PCR Master Mix No AmpErase UNG and 7.67 µl Nuclease-free water. Quantitative RT-PCR was performed using the Mx3005P QPCR (Stratagene, Waldbronn, Germany) and the thermal-cycling conditions consisted of 10 minutes at 95 °C, followed by 40 cycles with a profile of 15 seconds at 95 °C and 60 seconds at 60 °C. We investigated the presence of 11 different miRNAs in EVs secreted by porcine oviductal epithelial cells. MicroRNA primer sequences are shown in Table 1.

Table 1: Mature microRNA (miRNA) sequences

miRNA	Mature miRNA Sequence
hsa-mir-103	AGCAGCAUUGUACAGGGCUAUGA
hsa-let- 7a	UGAGGUAGUAGGUUGUAUAGUU
hsa-mir-19a	UGUGCAAAUCUAUGCAAAACUGA
hsa-miR-203	GUGAAAUGUUUAGGACCACUAG
hsa-mir-126	CAUUAUUACUUUUGGUACGCG
hsa-mir-19b	UGUGCAAAUCCAUGCAAAACUGA
hsa-mir-92	UAUUGCACUUGUCCCGGCCUG
RNU44	CCTGGATGATGATAGCAAATGCTGACTGAACATG AAGGTCTTAATTAGCTCTAACTGACT
hsa-mir-196a	UAGGUAGUUUCAUGUUGUUGGG
hsa-mir-326	CCUCUGGGCCCUUCCUCCAG
hsa-mir-23a	AUCACAUUGCCAGGGAUUUCC

2.6. Transmission Electron Microscopy

POEC and cell line derived EVs were prepared for Transmission Electron Microscopy (TEM) examination by negative stain. Purified EVs were transferred onto formvar/carbon-coated electron microscopy grids (Agar Scientific, Stansted, UK) and allowed to adsorb for 20 minutes. Next, EVs were fixed in Karnovsky fixative (Polysciences, Heidelberg, Germany) for 5 minutes, washed in sterile distilled water and contrasted in 2.5 % aqueous uranyl acetate (Agar Scientific). Images were obtained using a Tecnai 12 Spirit G2 Bio Twin transmission electron microscope (FEI, Hilsboro, Oregon, USA) equipped with Eagle 4k (FEI) and Veleta (Olympus, Hamberg, Germany) digital cameras.

2.7. Statistical analysis

GraphPad Prism 7 was used to perform the statistical analysis. Results were expressed as mean ± standard error of the mean (SEM). The size distribution of the EVs was expressed as mode ± SEM. Statistical analysis of EV data to compare two groups was performed using an unpaired two-tailed student's T-test. However, when more than two groups were compared, one-way or two-way ANOVA was performed. When comparing the EV size distributions, statistical analysis was performed using repeated measures ANOVA. All the experiments were performed on three biological replicates with either 3 or 4 technical replicates. $P<0.05$ was considered to be significant.

4.0. Results

4.1. Establishing SEC as a valid method for the isolation of EVs from POEC conditioned culture media

Following confirmation that a combination of ultracentrifugation and filtration was able to deplete serum-derived EVs 75-fold (Figure 1), POECs were cultured in complete cell culture medium supplemented with 10% EV-depleted FBS and SEC was performed to isolate the EVs from free proteins in the conditioned culture media. The concentration of EVs in each SEC column fraction was determined by NTA, with the majority of EVs eluting in fractions 7 to 20 (Figure 2). The diameter of EVs secreted by POECs as determined by NTA, was 50-250 nm and did not vary significantly between SEC fractions (Figure 3). In order to confirm that the particles detected by NTA were EVs, western blot analysis was performed to detect the presence of the EV markers CD63 and CD9. A pooled sample of EVs, consisting of SEC column fractions 7 to 12, showed strong bands for CD63 and faint bands for CD9, indicating that the isolated particles were indeed EVs (Figure 4).

To confirm that the SEC technique was able to isolate EVs from free-floating protein in the cell culture medium, each SEC fraction was assayed for protein concentration using the BCA assay. Protein was detected in SEC column fractions 13-20 (Figure 2). These findings were confirmed using gel electrophoresis with coomassie blue staining (not shown).

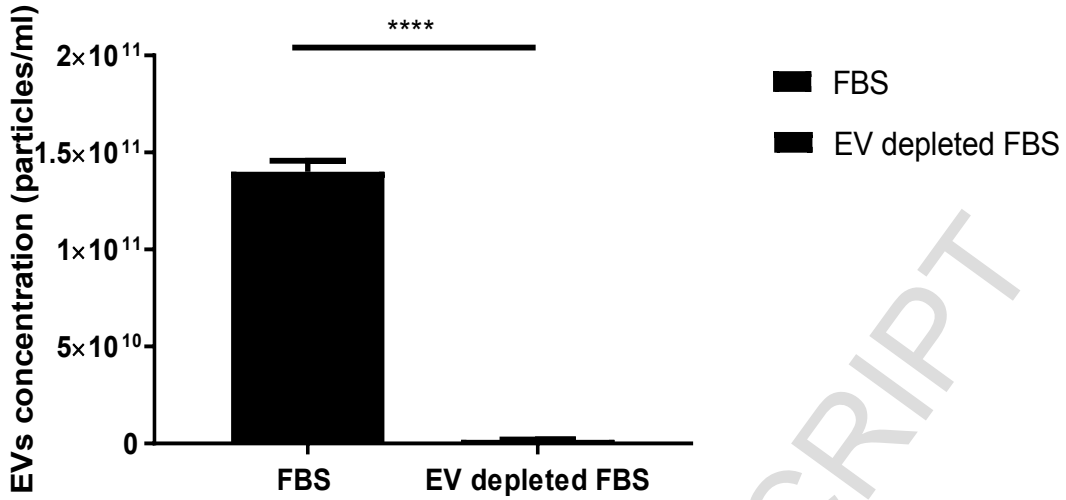

Figure 1: Extracellular vesicle (EV) concentration in normal foetal bovine serum (FBS) and EV-depleted FBS after ultracentrifugation. Nanoparticle tracking analysis (NTA) confirmed that there was a significant reduction in particle concentration in EV-depleted FBS after ultracentrifugation when compared to normal FBS. Experiments were performed in three biological replicates and three technical replicates. Error bars represent the standard error of the mean. **** P <0.0001.

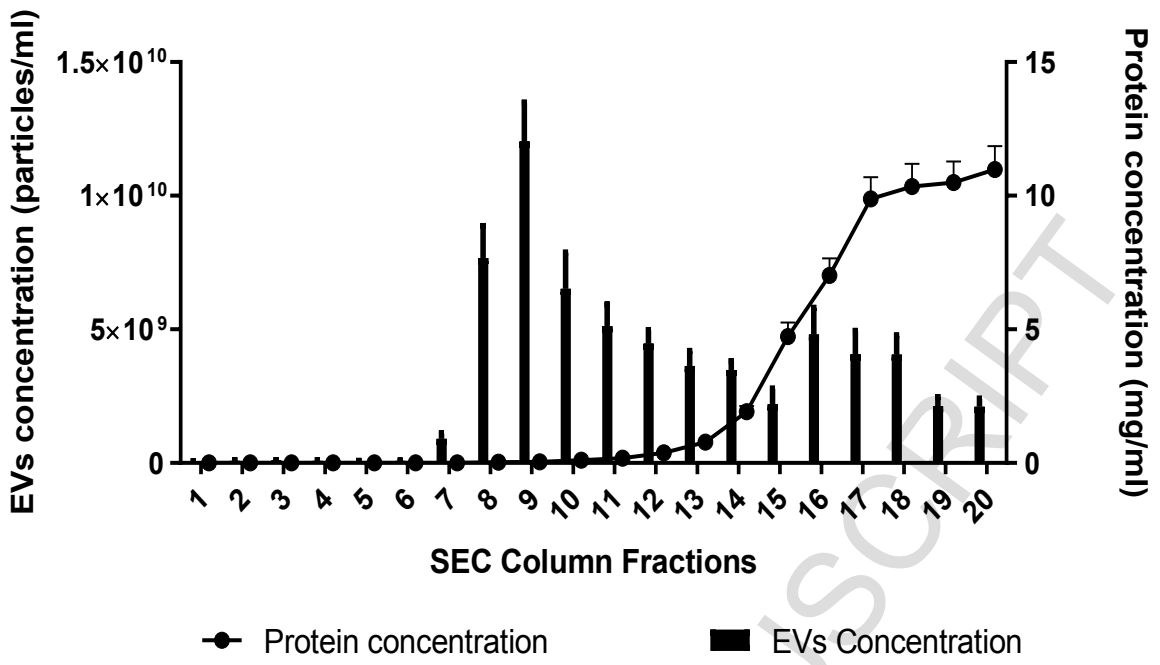

Figure 2: Characterising extracellular vesicles (EVs) secreted by porcine oviductal epithelial cells (POECs) and isolated using size exclusion chromatography (SEC). Conditioned culture media was collected once cells became 70% confluent. Twenty fractions of 500 µl were collected from the SEC column. The concentration of EVs in each SEC fraction was measured using nanoparticle tracking analysis (NTA). The protein concentration for each SEC fraction was measured using the Bicinchoninic acid assay (BCA) to determine if the SEC technique is capable of isolating EVs from free protein in culture media. The height of the bars represents the mean concentration (particles/ml) of EVs from three biological replicates and three technical replicates. The concentration of EVs in SEC fractions 1-6 ranged from 5.6 x 10^7/ml to 9.4 x 10^7/ml, while the majority of EVs eluted from the SEC column in fractions 7-20 with concentrations ranging from 9.0 x 10^8/ml to 1.2 x 10^{10}/ml. Circles represent the mean concentration of protein (mg/ml) in each SEC fraction from three biological replicates and three technical replicates. Error bars represent the standard error of the mean.

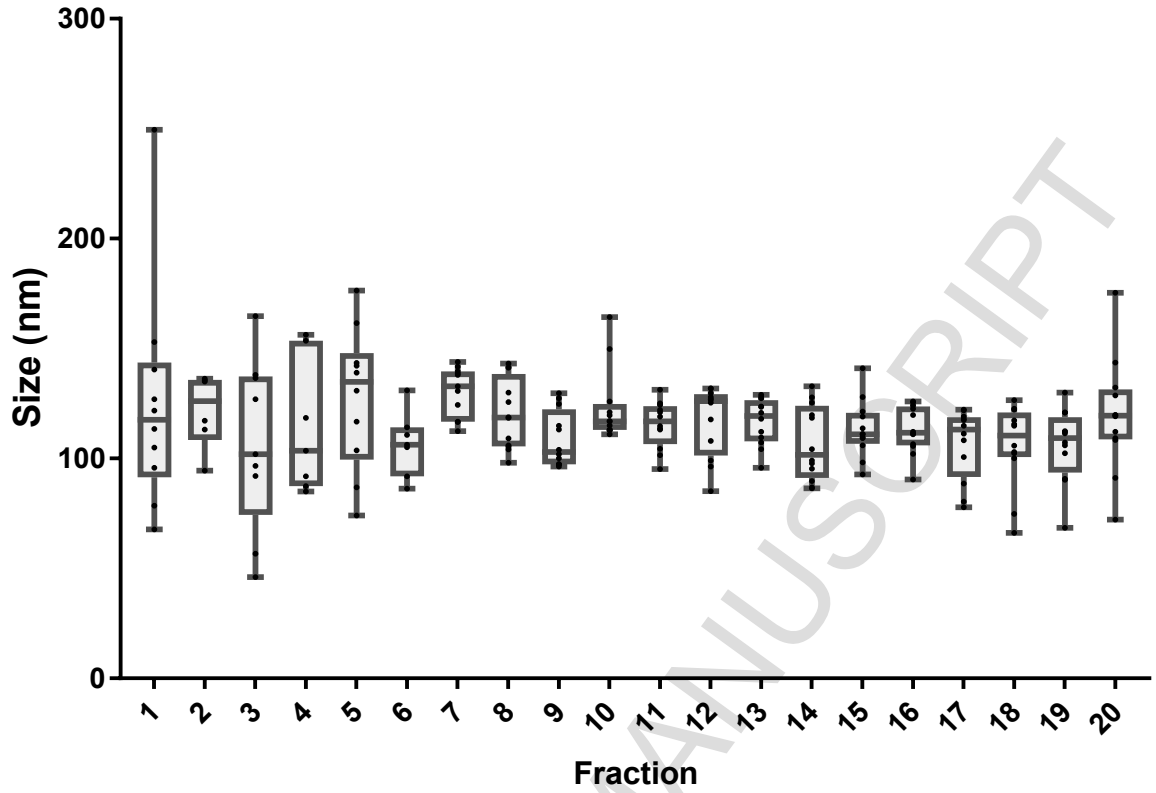

Figure 3: Characterising the size distribution of extracellular vesicles (EVs) secreted by porcine oviductal epithelial cells (POECs) and isolated by size exclusion chromatography (SEC). EV size in each of 20 SEC column fractions was determined using nanoparticle tracking analysis (NTA). Conditioned culture media was collected once cells became 70% confluent. Individual data points show the mode size of the EVs in each SEC column fraction, the top and bottom whiskers represent the 90th and 10th percentiles, the top and bottom boundaries of the boxes represent the 75th and 25th size percentiles and the median EV size is shown as a line in the box. EV size was measured in a minimum of three biological replicates and three technical replicates.

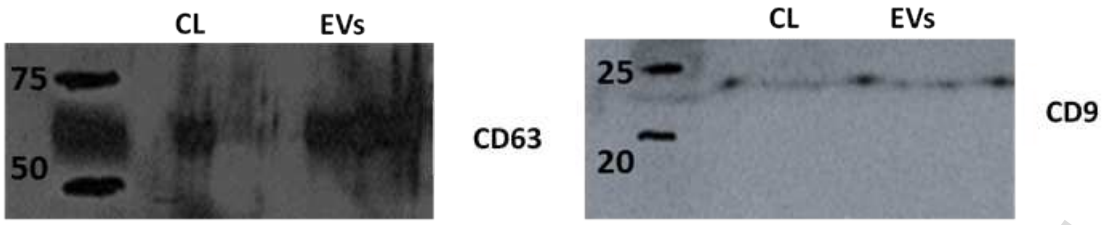

Figure 4: The presence of extracellular vesicles (EVs), secreted by porcine oviductal epithelial cells (POECs) and isolated using size exclusion chromatography (SEC), was confirmed using western blot analysis with the EV biomarkers CD63 and CD9. Western blotting was performed on a pool of EV samples isolated in SEC column fractions 7 to 12. Porcine oviductal epithelial cell lysate (CL) was used as a positive control. Molecular weight markers comprise the first lane of each blot.

4.2. Characterisation of EVs secreted by different cell types (reproductive versus non-reproductive and primary versus immortalised cell lines) after 24 hours and 48 hours of cell culture.

The characteristics of EVs secreted by POECs in primary culture, was compared to EVs secreted by immortalised cell lines of reproductive (RL95-2, Ishikawa) and non-reproductive origin (HEK293).

The concentration of EVs isolated by SEC (fractions 5 to 15) from conditioned media after 24 and 48 hours of cell culture, are shown in Figure 5. SEC fractions containing EVs secreted by POECs cultured for 24 hours, showed a bimodal distribution with peak concentrations of EVs eluting from the column in fractions 7-8 and fractions 10-12 (Figure 5a). In contrast, POECs cultured for 48 hours showed a single distribution of EV concentrations across SEC fractions with peak concentrations in fractions 7-9 (Figure 5a). SEC fractions containing EVs secreted by Ishikawa cells cultured for 24 hours, showed the presence of EVs in all fractions, with a marked increase in the concentration of EVs eluting at fraction 12 (Figure 5b). However, the majority of EVs secreted by Ishikawa cells cultured for 48 hours, eluted from the SEC column in fractions 7-12 (Figure 5b). SEC of EVs secreted by RL95-2 cells cultured for 24 hours, showed the presence of EVs in all fractions with peak EV concentrations in fractions 9-11 (Figure 5c), whereas EVs obtained from RL95-2 cells after 48 hours of culture, showed a bimodal distribution with maximum concentrations in fractions 7-9 and 11-13 (Figure 5c). SEC fractions containing EVs secreted by HEK293T cells showed bimodal distributions with peak EV concentrations at fractions 7-9 and 12-14 in samples taken from HEK293T cells after 24 hours of culture, and fractions 7-8 and 12-14 in samples taken from HEK293T cells after 48 hours of culture (Figure 5d).

The total number of EVs secreted by POECs and Ishikawa cells was time dependent, showing an increase in the number of EVs isolated from conditioned media over time ($p<0.001$; Figure 6). In contrast, the total number of EVs isolated from the conditioned media of HEK293T and RL95-2 cells in culture was not significantly different over time (Figure 6). The total number of EVs secreted per epithelial cell was calculated and showed no significant difference in the mean number of EVs produced per cell across all cell types at either 24 or 48 hours of culture (Figure 7). While the number of EVs produced per cell increased in POEC, RL95-2 and Ishikawa cell cultures over time, this increase did not prove to be significantly different (Figure 7).

The mode size distribution of EVs eluted in each SEC column fraction for each of the 4 cell types was significantly different following culture for either 24 hours or 48 hours (Figure 8). All evaluated SEC fractions, in all cell types, contained measurable EVs with a mode diameter of 80-160 nm (Figure 8). EVs secreted by the HEK293T cell line, after 24 and 48 hours of culture, eluting from the SEC column in fractions 5-10, exhibited similar mode diameters to those EVs assessed in POEC, Ishikawa and RL95-2 cells, however, HEK293T SEC fractions 11-15 contained EVs of significantly smaller diameter than those observed in EVs secreted by cells of reproductive origin (Figure 8).

The mean zeta potential of EVs secreted by POEC primary cell cultures was significantly different over time, with a mean (± standard error) EV zeta potential of -30.3 (± 0.744) mV at 24 hours, compared to -37.3 (± 2.66) mV at 48 hours ($p<0.0001$). These data are reflected in the POEC EV zeta potential frequency distributions, where electrokinetic potential exhibits a negative shift at 48 hours when compared with POEC EVs secreted at 24 hours (Figure 9a). All immortalised cell lines secreted EVs which showed no significant difference in zeta potential frequency distribution when cells were cultured for 24 or 48 hours (Figure 9).

TEM analysis was performed on purified EVs secreted by POEC, Ishikawa, RL95-2 and HEK293T cells. TEM revealed the presence of spherical vesicles with the artefactual cup-shape, measuring 30-170 nm in diameter (Figure 10). The majority of EVs were 30-100 nm in diameter, independent of their cell of origin.

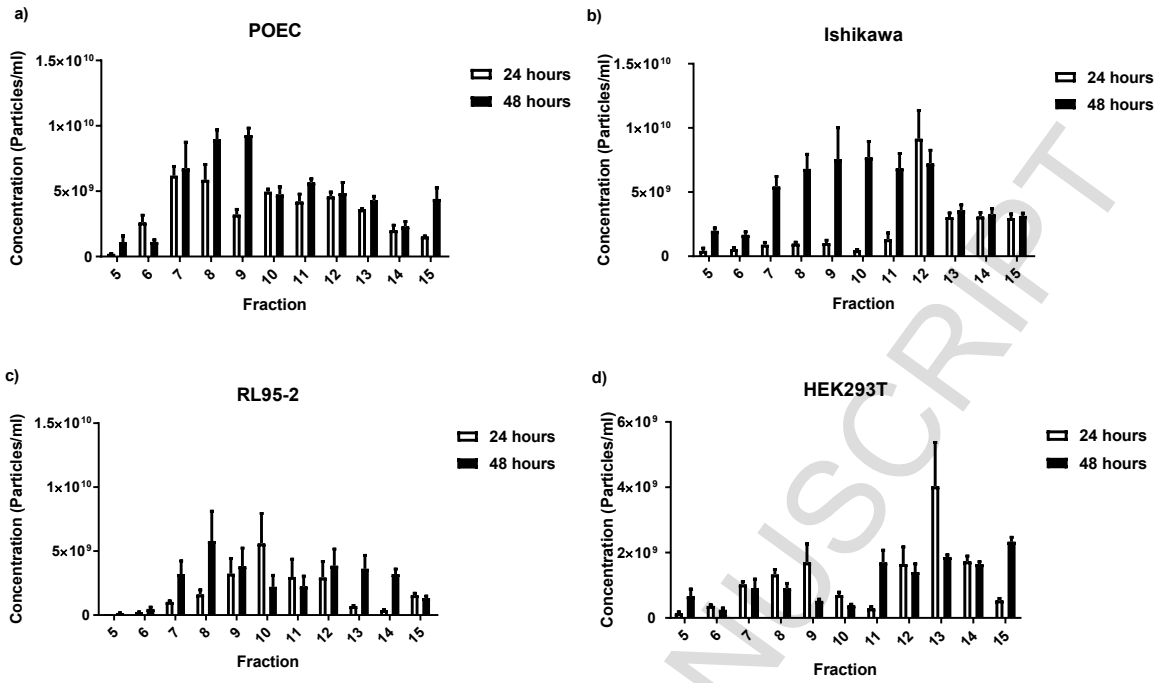

Figure 5: The concentration (particles per ml) of extracellular vesicles (EVs) produced by a) primary porcine oviductal epithelial cells (POEC); b) Ishikawa cells (human endometrial epithelial cell line); c) RL95-2 cells (human endometrial epithelial cell line); d) HEK293T cells (human embryonic kidney cell line) after 24 and 48 hours of culture in EV-depleted media. EVs were isolated from conditioned media by size exclusion chromatography (SEC) and assessed using nanoparticle tracking analysis (NTA). Data is shown as the mean (± standard error) concentration of EVs eluted in each SEC column fraction from three biological replicates and three technical replicates

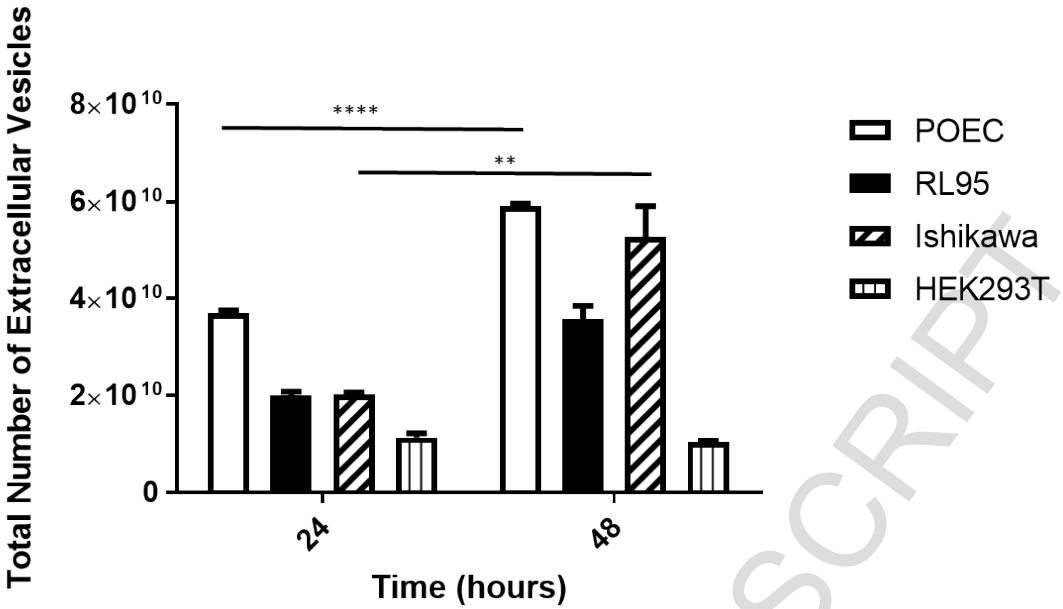

Figure 6: The total number of extracellular vesicles (EVs) produced by primary porcine oviductal epithelial cells (POECs), Ishikawa cells (human endometrial epithelial cell line), RL95-2 cells (human endometrial epithelial cell line) and HEK293T cells (human embryonic kidney cell line) after 24 and 48 hours of culture in EV-depleted media. EVs were isolated from conditioned media by size exclusion chromatography (SEC) and measured using nanoparticle tracking analysis (NTA). Data is shown as the mean (± standard error) number of EVs isolated from the conditioned cell culture media, from three biological replicates and three technical replicates. Statistical analysis were determined by t-test, **p=0.001 ****p<0.0001.

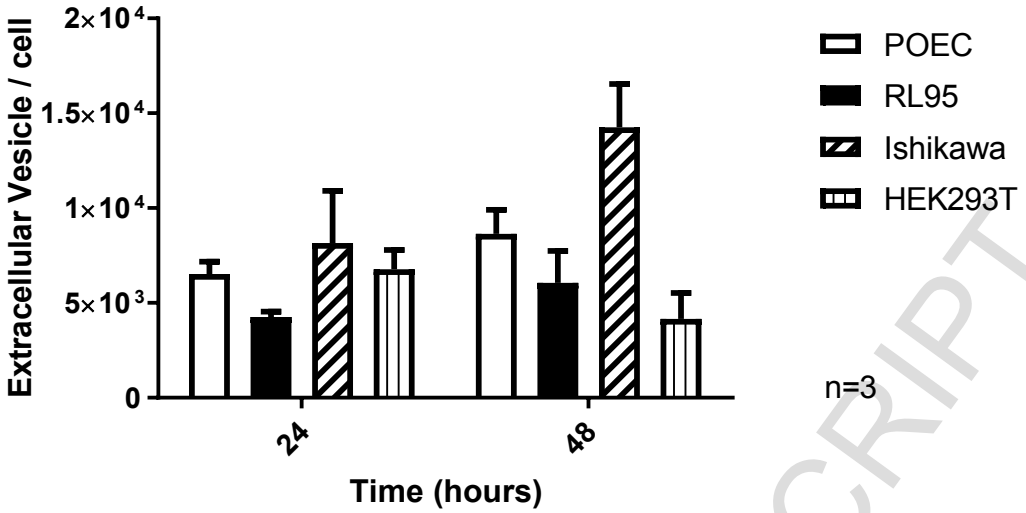

Figure 7: The total number of extracellular vesicles (EVs) secreted per cell, by primary porcine oviductal epithelial cells (POECs), Ishikawa cells (human endometrial epithelial cell line), RL95-2 cells (human endometrial epithelial cell line) and HEK293T cells (human embryonic kidney cell line) after 24 and 48 hours of culture in EV-depleted media. EVs were isolated from conditioned media by size exclusion chromatography (SEC) and measured using nanoparticle tracking analysis (NTA). Data is calculated as the mean (± standard error) total number of EVs isolated from the conditioned cell culture media per cell in culture, from three biological replicates and three technical replicates. Differences in the number of EVs secreted per cell over time showed no statistical significance.

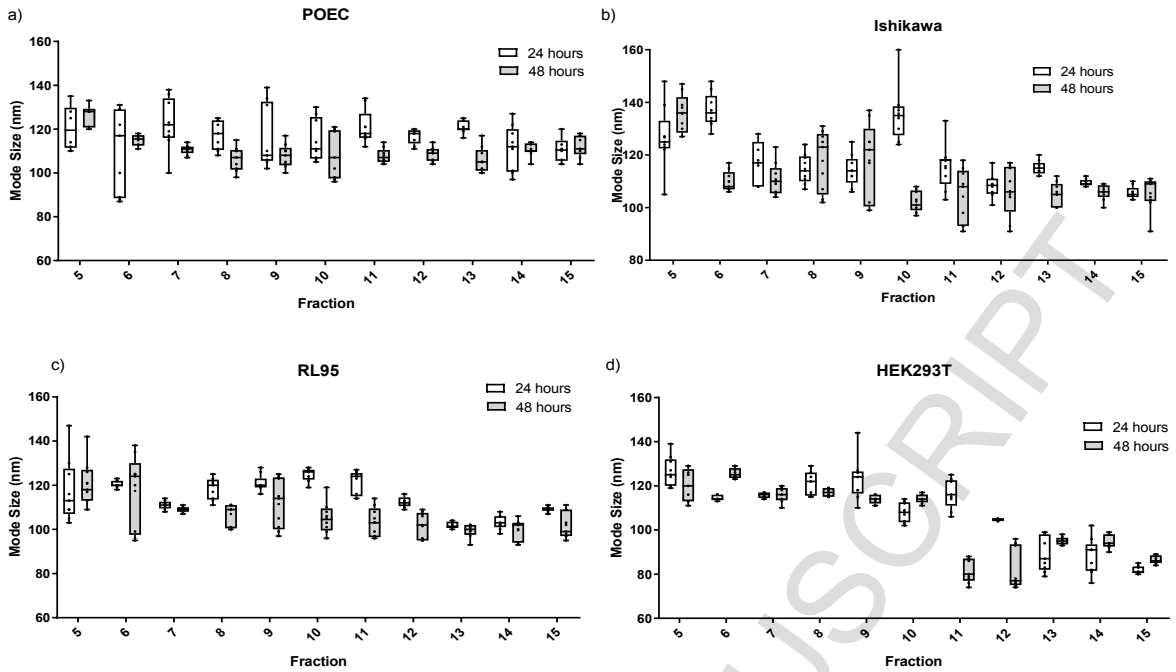

Figure 8: The size distribution of extracellular vesicles (EVs) secreted by primary porcine oviductal epithelial cells (POECs), Ishikawa cells (human endometrial epithelial cell line), RL95-2 cells (human endometrial epithelial cell line) and HEK293T cells (human embryonic kidney cell line) after 24 and 48 hours of culture in EV-depleted media. EVs were isolated from conditioned media by size exclusion chromatography (SEC) and measured using nanoparticle tracking analysis (NTA). Top and bottom boundaries of the box plots represent the 75th and 25th percentiles of the size distributions, top and bottom whiskers represent the 90th and 10th percentiles. The median of the data is shown as a line within the box. Measurement of EV sizes was performed in triplicate for each of three biological replicates.

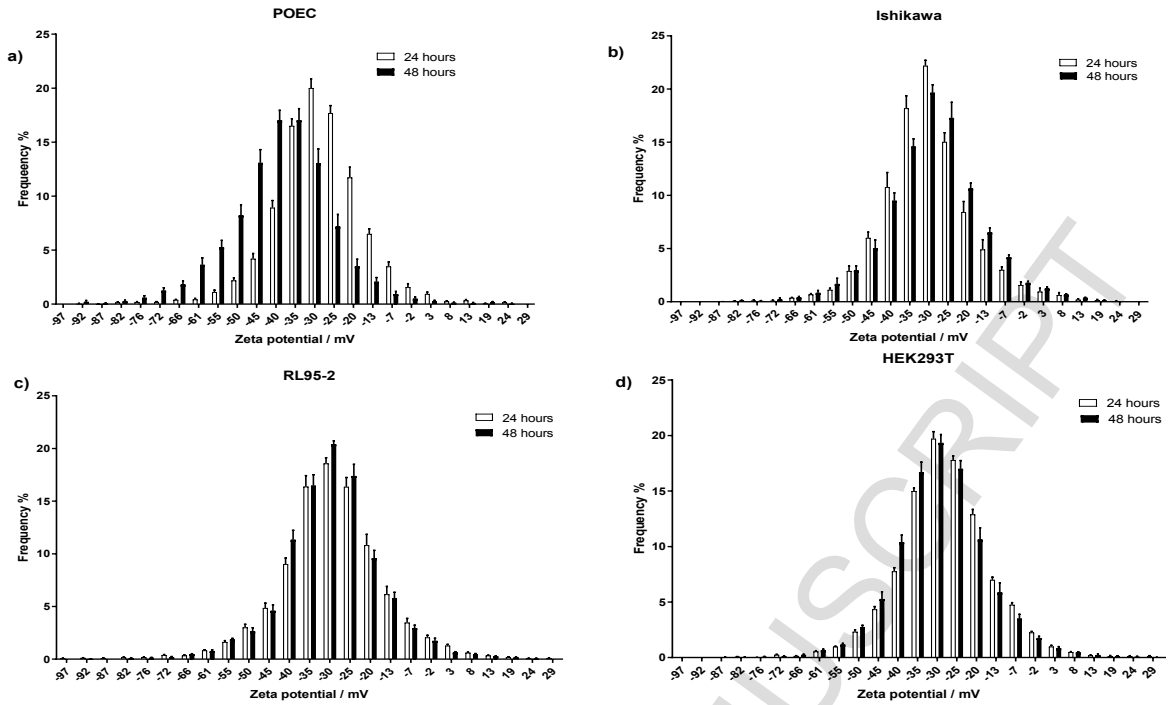

Figure 9: The zeta potential (ZP) percentage frequency distributions of extracellular vesicles (EVs) secreted by primary porcine oviductal epithelial cells (POECs), Ishikawa cells (human endometrial epithelial cell line), RL95-2 cells (human endometrial epithelial cell line) and HEK293T cells (human embryonic kidney cell line) after 24 and 48 hours of culture in EV-depleted media. EVs were isolated from conditioned media by size exclusion chromatography (SEC) and measured using nanoparticle tracking analysis (NTA). The ZP distributions of EVs derived from POECs after 48 hours of cell culture showed negative shifts compared with those EVs derived from POECs after 24 hours of culture ($p<0.0001$). In contrast, there were no significant differences in ZP for EVs derived from all immortalised cell lines after 24 and 48 hours of cell culture. These data represent the mean percentage of EVs detected with a specific ZP (±standard error) in four technical replicates for each of three biological replicates. Data were analysed using two-way ANOVA followed by Tukey *post-hoc* test.

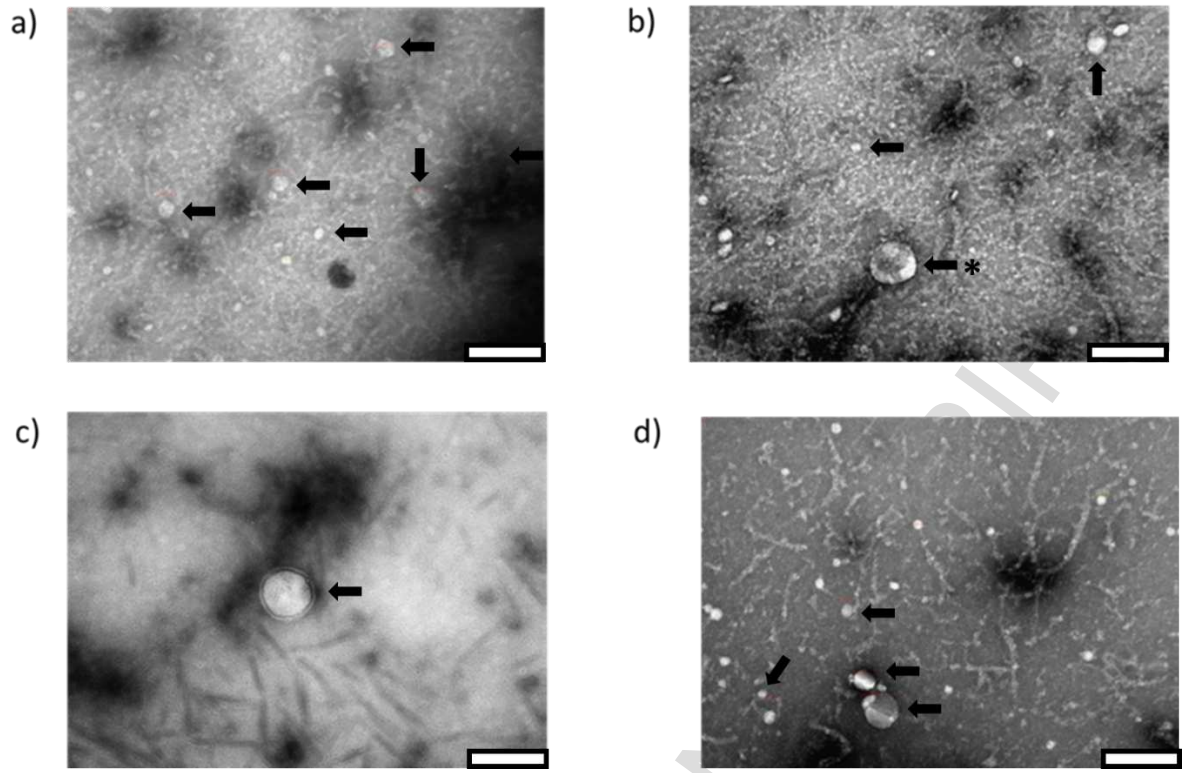

Figure 10: Extracellular vesicles (EVs) secreted by, (a) primary porcine oviductal epithelial cells (POECs), (b) Ishikawa cells (human endometrial epithelial cell line), (c) RL95-2 cells (human endometrial epithelial cell line) and (d) HEK293T cells (human embryonic kidney cell line), evaluated by transmission electron microscopy (TEM). TEM assessed EVs from a pool of SEC fractions (fractions 7 to 12), isolated from each cell type. The majority of EVs have a size range of 30-100 nm. Individual EVs are annotated using arrows. * identifies an EV exhibiting the artefactual cup-shape that is associated with EV TEM processing. Scale bar is 200 nm.

4.3. Characterisation of EVs secreted by oviductal epithelial cells from the ampulla (PAEC) and isthmus (PIEC) regions of the porcine oviduct

NTA data confirmed that the size distribution of EVs secreted by PAEC and PIEC were within the range previously reported for EVs isolated from POECs collected from whole porcine oviducts (Figure 11) and that there was no significant difference in the size of EVs secreted by epithelial cells from different regions of the oviduct. However, the mean number of EVs isolated from the conditioned media of PAECs in culture at 70% confluency ($2.2x10^{10}$ ± $1.61x10^{10}$) was significantly higher than the mean number of EVs isolated from cultured PIECs ($1.57x10^{10}$ ± $1.34x10^{10}$; p=0.008). In addition, EV surface charge properties, reflected by measurements of zeta potential, were significantly different between EVs isolated from the conditioned media of cultured PAECs (-36.86 ± 0.6341 mV) when compared to PIECs (-38.85 ± 0.0197 mV), indicating that EVs from different regions of the porcine oviduct might have distinct membrane characteristics and perhaps differing composition. This hypothesis is supported by data showing the frequency distribution of the zeta potential of individual EVs (Figure 12), where EVs originating from the isthmus region of the oviduct tend to exhibit a more negative zeta potential (mode of -40 mV) as compared to EVs secreted by epithelial cells in the ampulla (mode of -35 mV).

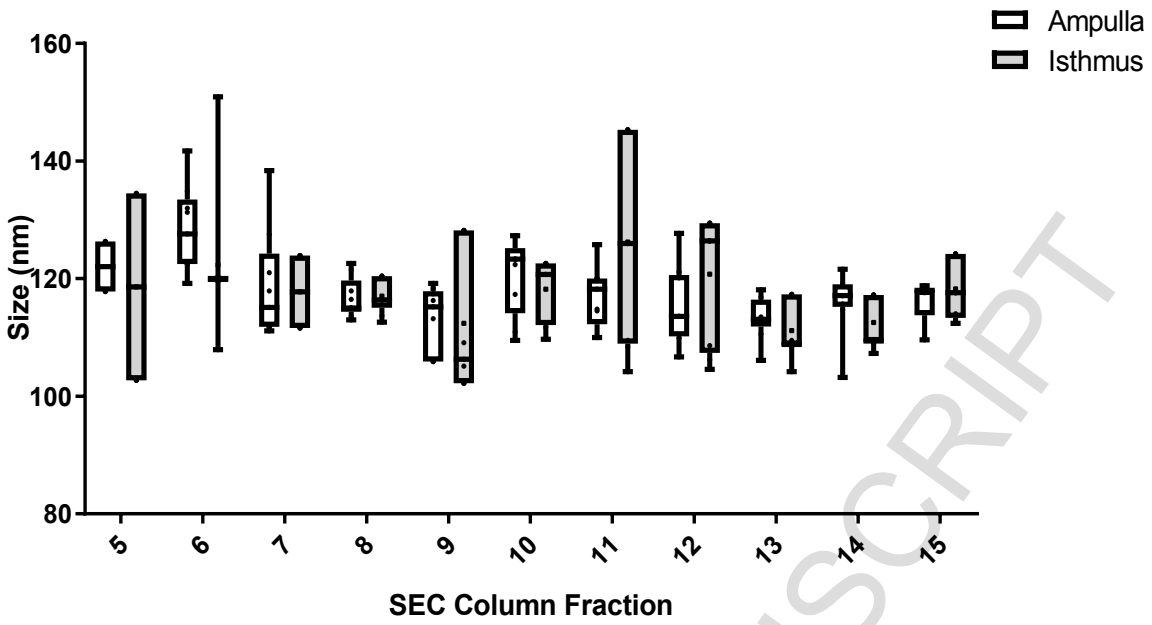

Figure 11: Size of extracellular vesicles (EVs) secreted by porcine epithelial cells harvested from the ampulla and isthmus regions of the oviduct. Conditioned culture media was collected 48 hours after the culture medium was changed to an EV-depleted FBS media. EVs were isolated from conditioned culture media using size exclusion chromatography (SEC) and EV size is shown for each of 15 SEC column fractions, as evaluated by nanoparticle tracking analysis (NTA). In the box plots, the top and bottom of the boxes indicate 75% and 25% of the size distribution, the bars show the median EV size, whiskers indicate the maximum and minimum EV size. Three technical assessments were carried out on each of three biological repeats.

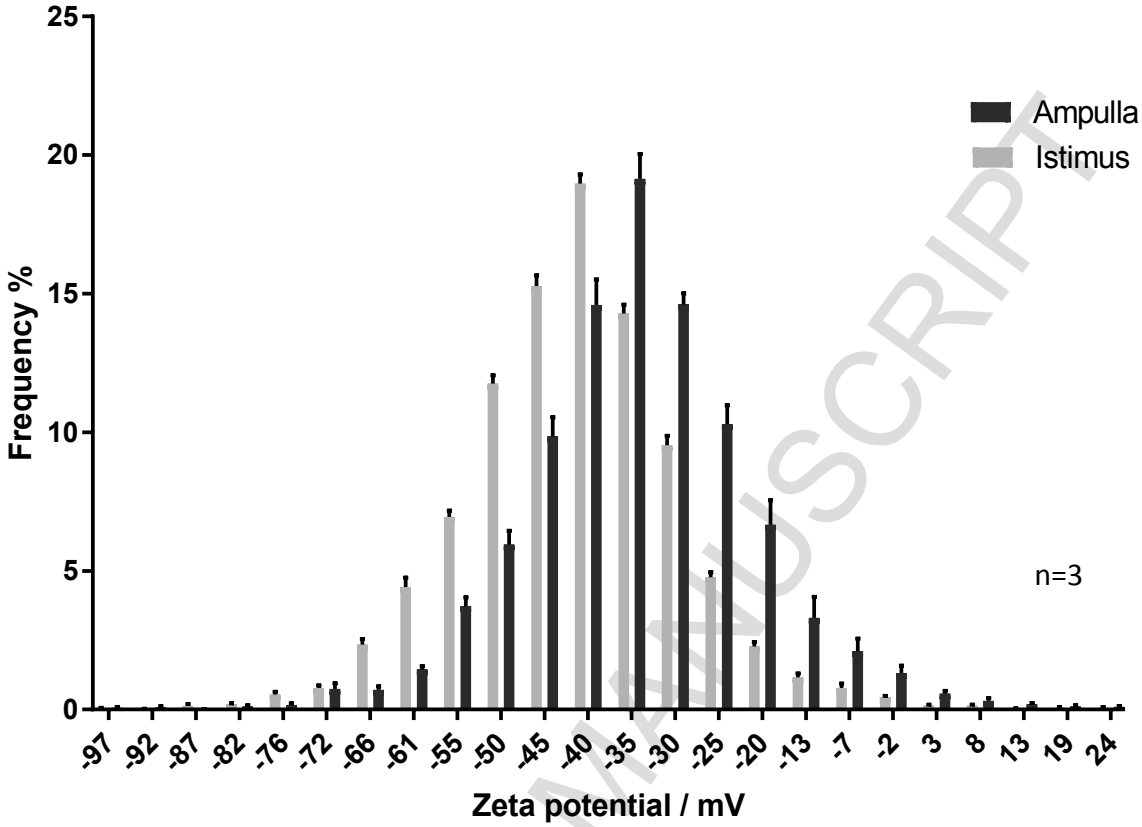

Figure 12: Variation in the electrokinetic charge, or zeta potential, of extracellular vesicles (EVs) secreted by primary porcine ampulla epithelial cells (PAEC) and primary porcine isthmus epithelial cells (PIEC) in culture as determined by nanoparticle tracking analysis (NTA). Conditioned culture media was collected 48 hours after the culture medium was changed to an EV-depleted FBS media and EVs were isolated by size exclusion chromatography (SEC). Data is shown as the mean (± standard error) percentage frequency of EV zeta potential from all EVs secreted by PAECs or PIECs. The zeta potential distribution of EVs secreted by PIECs tends to be more negative as compared to EVs obtained from PAECs. All experiments were performed on 3 biological repeats with 4 technical replications.

4.4. The identification of candidate miRNAs present in EVs secreted by POECs in vitro

4.4.1. Isolation of RNA from EVs using the miRCURY kit versus tri-Reagent

The concentration of RNA purified from EVs secreted by POEC cultures was 48782 ± 10781 pg/µl using the miRCURY kit, compared to 496 ± 251.6 pg/µl using tri-Reagent. As the concentration of RNA extracted from EVs using tri-Reagent was so low, we were not able to visualise the presence of either miRNA or small RNA in the electropherogram.

4.4.2. Quantitative RT-PCR validation of miRNA expression in EVs secreted by POECs in vitro.

For this analysis, RNA was extracted using the miRCURY kit. For each of 11 candidate miRNAs, mean expression data was calculated according to their quantification cycle (Ct) value. Six, of 11 candidate miRNAs were expressed in EVs secreted by POECs in vitro; miR-19b, miR-19a, miR-203, let-7a, miR-126 and miR-103; with Ct values ranging between 26-36 (Figure 13).

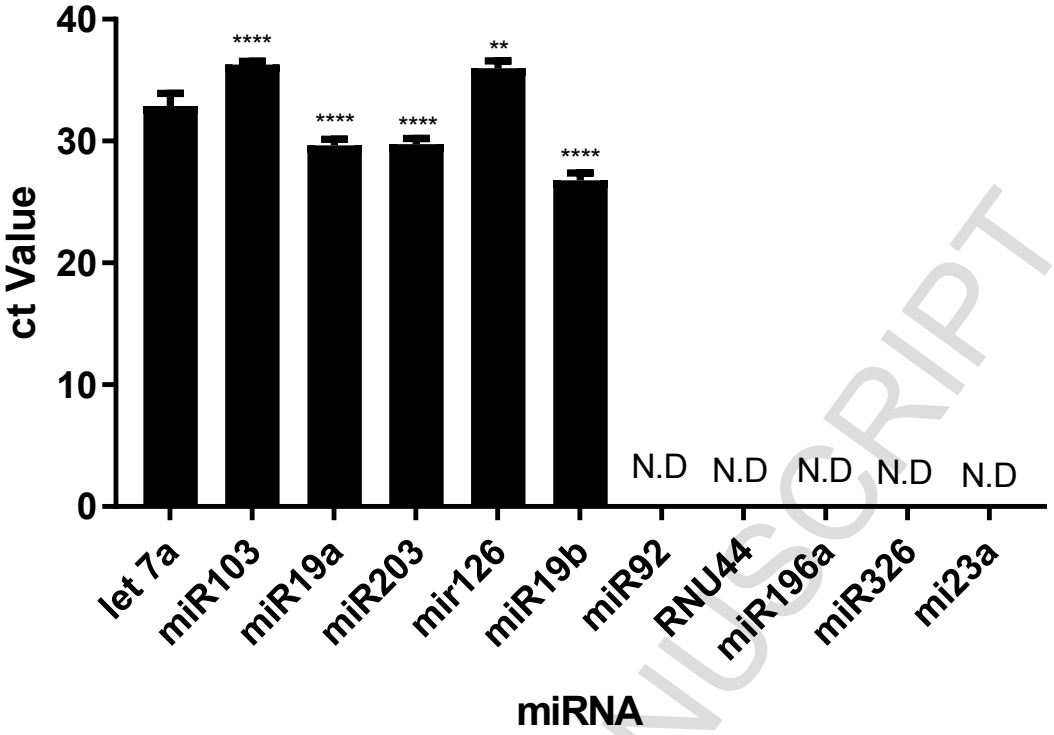

Figure 13: Quantitative real time PCR (qRT-PCR) analysis of microRNA (miRNA) isolated from extracellular vesicles (EVs) secreted by primary porcine oviductal epithelial cells (POECs). Of 11 miRNAs, only 6 showed expression in EVs secreted by POECs (let-7a, miR-103, miR-19a, miR-203, miR-126 and miR-19b). The height of the bar represents the mean (± standard error of the mean) of the quantification cycle (Ct) value for three biological replicates. **P=0.0019, **** P<0.0001, the statistical analysis was performed with one-way ANOVA with Sidak post hoc analysis. N.D: none detected.

5.0. Discussion

Extracellular vesicles (EVs) play pivotal roles in intercellular communication in all body systems, regulating both physiological and pathological processes [50-53]. This control of the intercellular environment is facilitated by the EV-mediated transport and delivery of a wide range of bioactive molecules including lipid, protein, DNA, RNA, mRNA and miRNA [54-56]. Many studies describe the roles of EVs in cell proliferation and differentiation in a broad range of cell types and tissues [57-59].

EVs play an essential role in cell-to-cell communications in the male and female reproductive tracts. To date, EVs have been identified in follicular fluid [55], seminal plasma [60], oviductal fluid [61] and uterine fluid [24]. In addition, EVs have been shown to be released by maternal reproductive tract epithelia [30, 62], oocytes [63], spermatozoa [38] and the embryo [64-65].

A multifaceted intercellular communication via EVs is thought to take place throughout the peri-conception period in order to facilitate successful fertilisation and subsequent pregnancy. For instance, during transit through the epididymis, spermatozoa acquire proteins and miRNAs, delivered by epididymal epithelial cell EVs, in order to undergo post-testicular maturation and acquisition of motility [66-68]. At ejaculation, spermatozoa are further exposed to EVs originating from the prostate gland. These prostasomes contain proteins, which, via their signal transduction, antioxidant and immuno-regulatory effects, are able to control the timing of spermatozoa capacitation and acrosome reaction [69-71].

The role of EVs in optimising gamete viability continues to be important in the female reproductive tract. Al-Dossary *et al.* [25] demonstrated that uterine and oviductal EVs are important modulators of spermatozoa maturation, preventing premature capacitation by maintaining Ca^{2+} homeostasis, via their delivery of plasma membrane Ca^{2+} ATPase 4a (PMCA4). Interestingly, the presence of gametes can elicit changes to the biochemistry of the female reproductive tract environment by stimulating novel gene expression in uterine epithelia [35-37]. These data indicate a potential role for EV-mediated miRNAs of gamete origin in the control of the maternal tract milieu. In addition to maintaining the viability of male gametes as they transit the female reproductive tract, EVs are known to influence the maturation and quality of the female gametes. Da Silveira *et al*. [55] and Santonocito *et al*. [72] demonstrated EV-mediated intercellular communication in the equine and human ovarian follicle respectively, identifying the presence of proteins and miRNAs known to target mechanisms controlling follicular growth and oocyte maturation, in EVs isolated from follicular fluid.

The essential role of EVs as vehicles for intercellular communication is further supported by evidence that following fertilisation, EV-mediated miRNAs of endometrial origin, have been predicted to act on targets that regulate embryo maturation and implantation [23]. Indeed, the female reproductive tract is able to respond to the presence of embryonic trophoblast cells, without any physical contact and prior to the establishment of stable attachment, by upregulating expression at the miRNA, transcriptomic and proteomic levels [65]. These EV-mediated communications between the maternal reproductive tract and the gametes and/or the embryo, might enable the female to act as a biological sensor that screens the gamete/embryo and then responds by modifying the oviductal environment to suit a specific need or selection pressure [5]. This idea is supported by the work of Lopera-Vasquez *et. al*. [62], who recently showed that EVs produced by bovine oviductal epithelial cells were able to improve the quality of blastocysts when added to embryo cultures.

Given the potential significance of EVs as vehicles for the transport of miRNAs between gametes and/or embryos and the female reproductive tract, we aimed to investigate methods for the extraction of RNA and miRNA from EVs. Despite their cellular origin, EV membranes are enriched with sphingomyelin and cholesterol, and contain less phosphatidylcholine than cellular membranes, making them more rigid and potentially more difficult to breach for RNA extraction [73-74]. Here, a column-based method and a phenol based method were compared for the extraction of RNA from EVs secreted by POECs. The quality of extracted EV RNA including purity, yield and size, and the analysis of small RNAs was determined. During generic RNA extraction analyses, the quality of RNA is assessed based on its Bioanalyser RNA integrity number (RIN) which is calculated based on 18s and 28s ribosomal RNA. Given the absence of ribosomal RNA in EVs, the RIN cannot be utilised to determine EV RNA quality. Instead, electropherograms of total RNA, showing size distribution in nucleotides (nt) versus fluorescence intensity, for both EV RNA purification methods were produced. Electropherograms generated from RNA extracted from EVs using the miRCURY kit showed the presence of miRNAs (15-40 nt) and small RNA, while the Tri-Reagent method was unable to recover adequate concentrations of EV-RNA for subsequent analysis. These findings are in agreement with those of Eldh *et al.* [74], who demonstrated that phenol-based methods of RNA extraction from EVs recovered low RNA yields when compared with column-based methods of RNA recovery.

In order to confirm the presence of miRNA in EVs secreted by POECs and to partially characterise the potential function of these EV mediated miRNAs, real-time PCR was performed using eleven candidate miRNAs. From these eleven miRNAs, six (let-7a, miR-19a, miR-203, miR-19b, miR-103 and miR-126), showed expression after real-time PCR, indicating that the miRCURY kit was able to successfully isolate miRNA from POEC EVs. Previous

studies in a number of different cell types, suggest that these six miRNAs are involved in membrane organisation [23], cell proliferation [75-76], cellular migration [77] and apoptosis [78]. Predicted target genes of miRNAs identified in endometrial EVs are known to play a role in the control of embryo implantation, regulating aspects of extracellular matrix interactions (let-7a, miR-19a) and VEGF signalling pathways [23]. It is not unreasonable to suggest that the miRNAs identified in POEC EVs during this study, might also be responsible for preparing the developing embryo for implantation as it transits the oviduct and moves into the endometrium.

The POEC-EV miRNAs identified here, are also expressed in EVs isolated from follicular fluid where they are known to target factors such as mitogen-activated protein kinase (MAPK) (miR-203) [72], transforming growth factor beta (TGFβ) (miR-19a) [55] and oestrogen signalling pathways (miR-19b) [79]. The MAPK pathway stimulates oviductal epithelial cell proliferation and is known to be associated with an increase in oviductal secretory activity, thus contributing to the maintenance and optimisation of the female tract milieu [80]. Interestingly, the presence of spermatozoa in the oviduct will stimulate oviductal epithelial cell MAPK pathways, indicating a role for these oviductal secretions in modulating sperm maturation within the female reproductive tract [81]. The activity of MAPK in the oviduct is further stimulated by the presence of oestrogen, suggesting a complementary role for miR-19b as it targets oviductal oestrogen signalling pathways [79]. Members of the TGFβ superfamily, including inhibin and activin, are expressed in the oviduct and are known to influence the female tract response to the presence of spermatozoa by supressing local innate immunity [82]. In addition, let-7a, miR-19b and miR-126 are involved in regulating inflammatory and innate immune responses, both of which are of pivotal importance for embryo development and implantation within the female reproductive tract [83].

Many recent investigations have utilised *in vitro* cell culture models in order to further clarify the essential role that EVs play in intercellular communications within the female reproductive tract. In order to draw useful conclusions, it is essential that these cell culture systems are fully optimised to facilitate the best possible production and recovery of EVs, while reflecting as much as possible, the *in vivo* environment. For instance, cells grown *in vitro* are usually supplemented with serum in order to support cell growth by providing nutrients and growth factors. Commercially available FBS contains high concentrations of EVs despite being filtered during processing [84]. Thus, in order to isolate EVs from cells of interest, it is crucial to remove any contaminating EVs from cell culture serum supplements. In addition, given that EVs are known to be vehicles for the transport of bioactive molecules, it is particularly important to minimise the contamination of experimental EVs with those EVs originating from serum supplements. Wei *et al*. [85] showed that FBS EVs contribute RNA to the culture system, which may influence cellular processes and cause misinterpretation of experimental results.

While there is commercial EV-depleted FBS available, it is very expensive as compared to normal sources of FBS. In this study, we have optimised a method for the EV depletion of FBS by ultracentrifugation. Ultracentrifugation has been performed previously to deplete EVs from FBS with variable success [86], using methods which manipulate several parameters including the duration and speed of centrifugation, and whether to centrifuge the FBS alone or following its addition to the culture medium. Here, EV-depleted FBS was produced by ultracentrifugation of FBS alone, at 100,000g at 4°C overnight, resulting in a 75-fold reduction in EV concentration as compared to the original source of FBS. Previous studies utilising ultracentrifugation to generate EV-depleted FBS, have applied significantly lower durations of centrifugation and as such, have been less successful in their elimination of EVs from the serum supplements. Eitan *et al.* [87] showed that, when centrifuged for 6 hours the reduction in FBS EV concentration was 7-fold, whereas with a 1 hour centrifugation, the FBS EV concentration was reduced just 2.2-fold. Shelke *et al.* [84], reported that ultracentrifugation of FBS for 1.5 hours was

insufficient to remove FBS EVs, when compared to an ultracentrifugation lasting 18 hours, further supporting our findings that a longer ultracentrifugation duration is required for the efficient depletion of EVs from FBS.

While it is important to remove contaminating EVs from serum supplements before they are added to cell culture systems, it is also imperative that we consider whether the use of EV-depleted FBS in cell cultures might have a detrimental effect on cell growth. The process of ultracentrifugation to produce EV-depleted FBS, will not only remove EVs, but might also eliminate non-EV material such as growth factors and nutrients that are important for the support of cell growth and proliferation. Eitan et al. [87] investigated serum derived EV involvement in cellular growth, showing that EVs isolated from FBS were able to increase cellular growth when added to cell culture medium. Aswad et al. [58], who showed that EVs in FBS are important regulators of cell proliferation in skeletal muscle cells, supported this work. Encouragingly, our data suggest that supplementation of POEC cultures with EV-depleted FBS, produced using our ultracentrifugation method, does not affect the number or proliferation rate of POECs. Light microscopy analysis showed that the number of POECs cultured in complete medium supplemented with 10% EV-depleted FBS was not significantly different to the number of POECs cultured in normal medium up to 72 hours of culture. In addition, the proliferation rate of POECs over 72 hours of culture remained consistent when the complete culture media was supplemented with either normal FBS or EV-depleted FBS, indicating that the removal of EVs from FBS did not affect POEC viability. While Eitan *et al.* [87] showed that a number of different cell types cultured in medium supplemented with EV-depleted FBS showed a significant reduction in cellular growth rates, they did not observe suppression of growth rate in human U87 glioblastoma cells. Hence, they suggest that any detrimental effect of using EV-depleted FBS in cell culture is cell and/or species dependent.

In this study, we aimed to evaluate SEC as a valuable method for the isolation of POEC derived EVs from conditioned cell culture medium. Recently, SEC has been reported to be an efficient method for the isolation of EVs with high purity and intact morphology. In addition, SEC is thought to have a rigorous ability to separate EVs based on size [88]. There are a number of different commercially available SEC column matrices including Sepharose CL-2B, Sepharose CL-4B, Sephacryl S-100 and Sephadex. Baranyai *et al*. [89] compared the efficiency of different SEC column matrices for the isolation of exosomes from blood plasma, showing that Sepharose CL-4B and Sephacryl S-400 were able to isolate exosomes in high purity without the presence of albumin. For our current investigations, SEC using Sepharose CL-2B combined with ultrafiltration, was successfully used to isolate EVs from conditioned cell culture medium. Interestingly, Baranyai *et al*. [89], published evidence that Sepharose CL-2B was unable to isolate exosomes efficiently from blood plasma, indicating that specific SEC matrices might be better suited for the recovery of EVs present in specific body fluids and/or cell culture media.

Our SEC approach generated two eluents from the conditioned media, first a series of EV-rich fractions, followed by distinct fractions of free-floating protein. Several detection techniques such as NTA, TEM, Western blot analysis and the BCA assay were used to characterise the fractions collected during the SEC elution. We have demonstrated that SEC was able to isolate EVs, as confirmed by the presence of the EV markers CD63 and CD9, from conditioned medium efficiently with high EV purity eluting from the SEC column in fractions 7 to 12. These fractions contained a high concentration of EVs with minimal protein concentration. In subsequent analyses, SEC fractions 7-12 were pooled to create a rich and concentrated sample of porcine oviductal EVs.

NTA is able to calculate EV size via the direct observation of Brownian motion in a fluid medium, visualised by a laser light scattering method and tracked over time. This enables the calculation of particle size using the Stokes-Einstein equation to determine the translational diffusion constant. In general, a large slow moving EV will cause a stronger light scattering pattern, than a small fast moving EV [41]. The size of EVs eluted from the SEC column were between 50-250 nm in all fractions. Despite previous suggestions that SEC might be able to separate EVs based on size, our data, and the results of Boing *et al*. [90], have demonstrated that there is no significant EV size distribution across different SEC fractions. It is possible that processing of the EV conditioned media by differential centrifugation and ultrafiltration, prior to SEC sample loading, has already removed larger (cell debris) and smaller (free-floating protein) particles from the culture medium [91-92], leaving only mid-range EVs to travel through the SEC column. Nordin et al. [93], who showed that when ultrafiltration is combined with SEC, more particles with a similar size distribution were recovered from the column, support this hypothesis. Future investigations might also consider manipulating the ZetaView® pre-acquisition parameters in order to detect particles of a larger size in each SEC fraction. Our ZetaView® measurement parameters (sensitivity 85; shutter value 70, corresponding to an exposure time of 15 ms; frame rate 30 frames per second) are set to detect small particles (50-250 nm) with weak light scattering, which correspond with previously published EV size data. It is possible that any larger non-EV particles that were present in our SEC fractions were not detected by the ZetaView NTA evaluation. In order to detect the presence of larger particles with strong light scattering, the ZetaView® sensitivity should be decreased, shutter values increased (corresponding to a decreased exposure time) and frame rate increased.

As well as recovering EVs of expected size, in agreement with previous studies, we have demonstrated that EVs isolated using SEC are morphologically intact as confirmed by TEM [90, 94].

During these investigations, we have characterised EVs secreted by epithelial cells of reproductive origin, (POEC, Ishikawa and RL95-2) and non-reproductive origin (HEK293T). Furthermore, we have investigated whether the characteristics of EVs secreted by these different cell types altered over time in cell culture. For all reproductive cell types (POEC, Ishikawa and RL95-2), the number of EVs secreted increased over time in culture, as epithelial cell number also increased. In contrast to our reproductive cells, HEK293T epithelial cell cultures showed a decrease in the total concentration of EVs secreted over time, independent of cell number. Hurwitz *et al*. [95], performed a similar study with HEK293T cells, where they determined that the concentration of EVs produced related to the degree of cell culture confluency. In addition, Riches *et al.* [96], showed that the total number of EVs secreted by normal mammary epithelial cells after 24 hours of culture, was less than the number of EVs collected from two consecutive 12 hour cultures, suggesting that the concentration of EVs secreted is not dependent on cell number, but rather on the stage of cellular development. It is also important to consider that as vehicles for intercellular communication, EVs will not only be produced by their cells of origin, but will also be taken up by their recipient cellular targets. Indeed, several groups have demonstrated that as well as secreting EVs, cells in an *in vitro* culture system will uptake EVs via a variety of different mechanisms [97-99]. For instance, Escrevant *et al.* [98] demonstrated that different endocytic pathways are involved in the uptake of exosomes secreted by the ovarian cancer cell line SKOV3.

In addition to EV concentration, NTA determined the size distribution of all experimental epithelial cell EVs as between 70 to 140 nm, complying with previously published data for expected EV size parameters [11]. These data indicate a slightly larger EV size than is observed with TEM. Electron microscopy is the standard visual method for defining the size and morphology of EVs since the optical microscope cannot identify particle sizes smaller than 300 nm [41-43, 100-102]. EV size measurements obtained via TEM are generally smaller than those obtained with NTA, due to particle dehydration following exposure to the high vacuum,

anhydrous atmosphere required for TEM assessment [102]. Conversely, NTA evaluates EVs in a solution, maintaining their hydrodynamic diameter and producing a more reliable indication of their true size [41].

Recently, there has been an increase in the number of studies investigating the biological properties and functions of EVs. Despite this increased level of interest, the physical properties of EVs, including their electrochemical characteristics, remain unclear. Information regarding EV surface charge is important as it plays an essential role in both EV-cell and EV-matrix interactions [103]. Furthermore, Zeta potential provides a vital indication of the stability of EVs in solution in terms of flocculation, dispersion and aggregation (Figure 13) [44]. Nanoparticles considered to be electrically 'neutral', with a Zeta potential between -10mV and +10Mv, tend to form aggregates when in solution. Whereas nanoparticles of Zeta potential greater than +30mV or less than -30Mv, are known to be more stable in solution [104]. As well as influencing the behaviour of populations of EVs in solution, it has been reported that Zeta potential is a useful indicator of the ability of nanoparticles to interact with their target cells, influencing cell adhesion, agglutination and cellular activation [105-108].

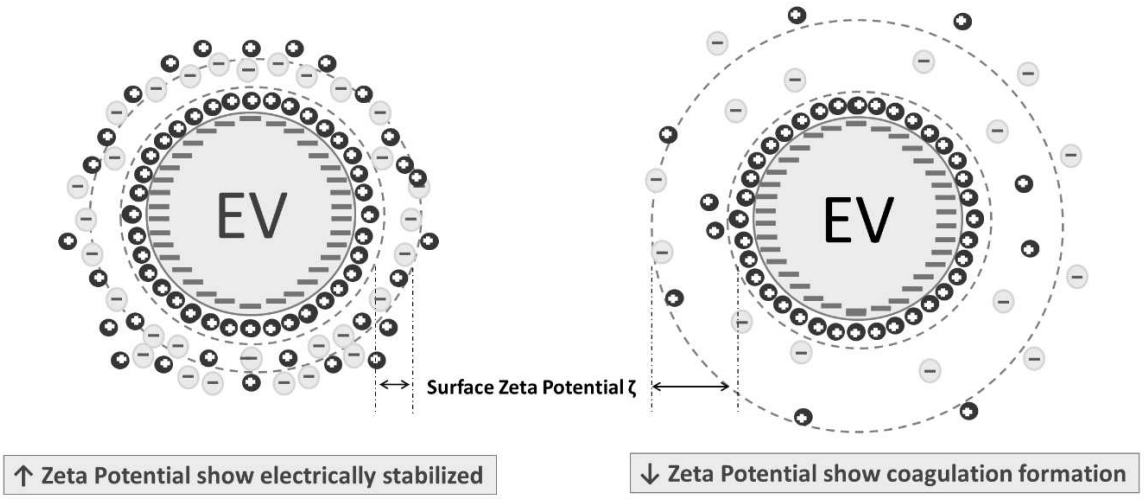

Figure 14: Zeta Potential, measured in mV, is the electrokinetic potential of the interfacial region between the extracellular vesicle (EV) surface and the aqueous environment [45]. Zeta potential is a fundamental parameter known to affect the stability of particles in solution [47]. EVs with low stability (exhibiting a low zeta potential between -20 to +20 mV), will be expected to fuse or form aggregates. The zeta potential, and hence the stability of an EV in solution, is affected by the temperature, pH and ionic strength of the aqueous medium [45, 48]. In addition, zeta potential is affected by, and is a reflection of, the surface charge of the EV and thus the physiological makeup of the plasma membrane [48]. In cell biology, zeta potential has been used to study biological activation, agglutination and adhesion [49].

Our results showed that only EVs originating from primary cell cultures exhibit differing characteristics over time, whereas those EVs secreted by immortalised cell lines show a more consistent series of descriptors. Data shown herein indicate that a correlation exists between EV zeta potential and the maturational status of their cells of origin. This hypothesis is supported by Kato *et al.* [109] who reported a strong correlation between the zeta potential of

exosomes and the type of cell from which they were secreted. Our findings, and the data produced by Kato *et al*. [109], can be explained by understanding the formation and secretion of EVs by cells. It is known that EVs defined as microvesicles are most likely secreted by direct budding from the cellular plasma membrane [15, 110-112]. Hence, EVs are likely to contain the same membrane properties as their cells of origin. The surface charge of the cell is known to reflect cellular function and is dependent on both plasma membrane composition and the physiological conditions within the cell [48, 113]. A number of intracellular pathways involving cell proliferation, cell adhesion, cell differentiation and cellular apoptosis, are modulated by plasma membrane electrical potential [113-116]. As primary *in vitro* cell cultures are still undergoing the process of differentiation, it is not unreasonable to assume that their properties, including their zeta potential, will continue to be modified over time. Whereas, immortalised cell lines in culture are fully differentiated and their physiological properties will remain consistent. As the EV plasma membrane reflects the plasma membrane of its cell of origin, we might expect the EVs secreted from cells in primary culture to be subject to change, as that cell differentiates over time, and the EVs secreted by an immortalised cell line to be more consistent over time in culture [117].

In this series of experiments, we have demonstrated that the ZetaView instrument is able to reliably evaluate the size, concentration and zeta potential of individual EVs secreted by epithelial cells in culture. Furthermore, we have shown that the zeta potential distribution of EVs secreted by different epithelial cell types, differs over time, in primary culture systems, but not in immortalised cell line cultures. While zeta potential is a valuable tool for the evaluation of EV surface charge, further research is required to investigate how EV zeta potential is influenced by altered plasma membrane composition and biochemical change within its cell of origin.

Given that, the characteristics of EVs differ dependant on their cell of origin, and that different regions of the oviduct are functionally differentiated, it is important to clarify how the secretion and characteristics of oviductal EVs might vary between the ampullary and isthmus regions of the oviduct. NTA analysis of EV concentration showed that significantly more EVs are secreted by epithelial cells isolated from the ampullary region of the oviduct (PAECs), when compared to the isthmus (PIECs). We found no significant difference in the size of EVs produced across all regions of the oviduct. Interestingly, Lopera-Vasquez *et al*. [26] showed that in the bovine oviduct, epithelial cells isolated from the isthmus produced smaller EVs as compared to epithelial cells from the ampulla, suggesting that the pattern of EV secretion between the ampulla and isthmus might be species dependent. In support of our suggestion that distinct populations of EVs are produced by both the oviductal isthmus and ampulla, we established that EVs from different regions of the oviduct have significantly different zeta potential measurements, indicating that their surface characteristics and potentially membrane composition are different. Our data showed that the zeta potential of EVs secreted by PIECs was less negative as compared to EVs secreted by PAECs. Given that EVs form by outward budding of the plasma membrane, it is not unreasonable to assume that the functional and morphological variation identified between oviductal epithelial cells from the isthmus and ampulla, might be reflected in their EV surface parameters. The further clarification of how EV characteristics change throughout the oviduct will allow us to understand how intercellular communication takes place and ultimately may provide us with useful tools with which to improve the success of fertilisation and pre-implantation embryo development.

6.0. Conclusion

In conclusion, this study has confirmed the presence of miRNAs (miR-103, let-7a, miR-19a, miR-203, miR-126, miR-19b) in EVs secreted by cultured POECs. These miRNAs are known

to be involved in cell proliferation, innate immune responses, apoptosis and cellular migration, potentially acting on the periconception events taking place in the oviduct, which result in the successful establishment of pregnancy. We have demonstrated that NTA can successfully measure the concentration and size of EVs secreted by different epithelial cell types. Interestingly, the concentration of EVs secreted by POEC and Ishikawa cells seems to be dependent on their time in culture suggesting that the characteristics of EVs secreted by cells *in vitro*, relate to the functional and/or developmental status of their cells of origin. In addition, we showed that the surface electrokinetic charge (zeta potential) of EVs derived from primary epithelial cell cultures was different as compared to EVs secreted by cultured epithelial cell lines, suggesting that the molecular composition of the EV plasma membrane reflects subtle changes in the biochemistry of its cell of origin. Furthermore, we have determined that the electrokinetic surface characteristics of EVs differ between epithelial cells from functionally distinct regions of the oviduct, reinforcing the idea that EVs have specific and targeted roles in intercellular communications in the female reproductive tract. Future investigations will not only determine how EV zeta potential might reflect the biochemical properties of different EV populations produced by a variety of cell types, but will also improve our knowledge of the role of EVs in reproduction, with the view to identify factors that might influence the success of assisted reproductive technologies.

Acknowledgments

This research was funded by the government of Malaysia and the European Union through (1) the Corporation in Science and Technology (COST) Action CA16119 ‘In vitro 3-D total cell guidance and fitness’; (2) the COST Action FA1201 ‘Epigenetics and periconception environment’; (3) the Coordination and Support Action of the Horizon 2020 programme, grant No. 692299 ‘Scientific Excellence in Animal Reproductive Medicine and Embryo Technology’;

(4) grant No. 668989, and (5) the Polish Ministry of Science and Higher Education, Project: Scientific Consortium 'Healthy Animal – Safe food'. The authors wish to thank Particle Metrix, Germany for their advice and support of our research.

Author Roles

N.J.A. contributed to the study design, performed the literature search and acquired, analysed and interpreted the data. LMT contributed to the study design, performed the literature search, analysed and interpreted the data, wrote the manuscript, performed revisions and critically discussed the complete manuscript before submission. KJW, AM, SB, SE and AA acquired and analysed the data. AF and SH contributed to the conception and design of the study, performed revisions and critically discussed the complete manuscript before giving final approval of content before submission.

References

[1] Fazeli A, Holt WV. Cross talk during the periconception period. Theriogenology 2016; 86:438-442.

[2] Holt WV, Fazeli A. Do sperm possess a molecular passport? Mechanistic insights into sperm selection in the female reproductive tract. Molecular human reproduction 2015; 21:491-501.

[3] Fazeli A, Duncan AE, Watson PF, Holt WV. Sperm-oviduct interaction: induction of capacitation and preferential binding of uncapacitated spermatozoa to oviductal epithelial cells in porcine species. Biology of reproduction 1999; 60:879-86.

[4] Tienthai P, Johannisson A, Rodriguez-Martinez H. Sperm capacitation in the porcine oviduct. Animal reproduction science 2004; 80:131-46.

[5] Thurston LM, Holt WV, Fazeli A. Battle of the Sexes: How the selection of spermatozoa in the female reproductive tract manipulates the sex ratio of offspring. In Legato MJ ed., Principles of Gender Specific Medicine 2017, Third Edition, Elsevier.

[6] Talevi R , Gualtieri R. Sulfated glycoconjugates are powerful modulators of bovine sperm adhesion and release from the oviductal epithelium in vitro. Biology of reproduction 2001; 64:491-8.

[7] Liberda J, Manaskova P, Prelovska L, Ticha M, Jonakova V. Saccharide-mediated interactions of boar sperm surface proteins with components of the porcine oviduct. Journal of reproductive immunology 2006; 71:112-25.

[8] Talevi R, Zagami M, Castaldo M, Gualtieri R. Redox regulation of sperm surface thiols modulates adhesion to the fallopian tube epithelium. Biology of reproduction 2007; 76:728-35.

[9] Gualtieri R, Mollo V, Barbato V, Talevi R. Ability of sulfated glycoconjugates and disulfide-reductants to release bovine epididymal sperm bound to the oviductal epithelium in vitro. Theriogenology 2010; 73:1037-43.

[10] Kadirvel G, Machado SA, Korneli C. Porcine sperm bind to specific 6-sialylated biantennary glycans to form the oviduct reservoir. Biology of reproduction 2012; 87:147.

[11] Thery C, Zitvogel L, Amigorena S. Exosomes: composition, biogenesis and function. Nat Rev Immunol 2002; 2:569-579.

[12] Mulcahy LA, Pink RC, Carter DR. Routes and mechanisms of extracellular vesicle uptake. J Extracell Vesicles 2014; 3

[13] Yanez-Mo M, Siljander PR, Andreu Z, Zavec AB, Borras FE, Buzas EI, Buzas K, Casal E, Cappello F, Carvalho J, Colas E, Cordeiro-da Silva A, Fais S, Falcon-Perez JM, Ghobrial IM, Giebel B, Gimona M, Graner M, Gursel I, Gursel M, Heegaard NH, Hendrix A, Kierulf P, Kokubun K, Kosanovic M, Kralj-Iglic V, Kramer-Albers EM, Laitinen S, Lasser C, Lener T, Ligeti E, Line A, Lipps G, Llorente A, Lotvall J, Mancek-Keber M, Marcilla A, Mittelbrunn M, Nazarenko I, Nolte-'t Hoen EN, Nyman TA, O'Driscoll L, Olivan M, Oliveira C, Pallinger E, Del Portillo HA, Reventos J, Rigau M, Rohde E, Sammar M, Sanchez-Madrid F, Santarem N, Schallmoser K, Ostenfeld MS, Stoorvogel W, Stukelj R, Van der Grein SG, Vasconcelos MH, Wauben MH, De Wever O. Biological properties of extracellular vesicles and their physiological functions. J Extracell Vesicles 2015; 4:27066.

[14] Tkach M, Thery C. Communication by Extracellular Vesicles: Where We Are and Where We Need to Go. Cell 2016; 164:1226-1232.

[15] Colombo M, Raposo G, Thery C. Biogenesis, secretion, and intercellular interactions of exosomes and other extracellular vesicles. Annu Rev Cell Dev Biol 2014; 30:255-289.

[16] Castoldi M, Kordes C, Sawitza I, Haussinger D. Isolation and characterization of vesicular and non-vesicular microRNAs circulating in sera of partially hepatectomized rats. Sci Rep 2016; 6:31869.

[17] Kowal J, Arras G, Colombo M, Jouve M, Morath JP, Primdal-Bengtson B, Dingli F, Loew D, Tkach M, Thery C. Proteomic comparison defines novel markers to characterize heterogeneous populations of extracellular vesicle subtypes. Proc Natl Acad Sci USA 2016; 113:e968-977.

[18] Willms E, Johansson HJ, Mager I, Lee Y, Blomberg KE, Sadik M, Alaarg A, Smith CI, Lehtio J, El Andaloussi S, Wood MJ, Vader P. Cells release subpopulations of exosomes with distinct molecular and biological properties. Sci Rep 2016; 6:22519.

[19] Caby MP, Lankar D, Vincendeau-Scherrer C, Raposo G, Bonnerot C. Exosomal-like vesicles are present in human blood plasma. Int. Immunol 2005; 17:879-887.

[20] Kim DK, Kang B, Kim OY, Choi DS, Lee J, Kim SR, Go G, Yoon YJ, Kim LH, Jang SC, Park KS, Choi EJ, Kim KP, Desiderio DM, Kim YK, Lotvall J, Hwang D, Gho YS. EVpedia: an integrated database of high-throughput data for systemic analyses of extracellular vesicles. J Extracell Vesicles 2013; 2.

[21] Buzas EI, Gyorgy B, Nagy G, Falus A, Gay S. Emerging role of extracellular vesicles in inflammatory diseases. Nat Rev Rheumatol 2014; 10:356-364.

[22] Aalberts M, Sostaric E, Wubbolts R, Wauben MW, Nolte-'t Hoen EN, Gadella BM, Stout TA, Stoorvogel W. Spermatozoa recruit prostasomes in response to capacitation induction. Biochim Biophys Acta 1013; 1834 2326-35.

[23] Ng YH, Rome S, Jalabert A, Forterre A, Singh H, Hincks CL, Salamonsen LA. Endometrial exosomes/microvesicles in the uterine microenvironment: a new paradigm for embryo-endometrial cross talk at implantation. PLoS ONE 2013; 8:e58502.

[24] Burns G, Brooks K, Wildung M, Navakanitworakul R, Christenson LK, Spencer TE. Extracellular vesicles in luminal fluid of the ovine uterus. PLoS One 2014; 9:e90913.

[25] Al-Dossary AA, Strehler EE, Martin-Deleon PA. Expression and seretion of plasma membrane Ca2+-APTase 4a (PMCA4a) during murine estrus:association with oviductal exosomes and uptake in sperm. PLoS ONE 2013; 8 e80181.

[26] Lopera-Vasquez R, Hamdi M, Maillo V, Gutierrez-Adan A, Bermejo-Alvarez P, Ramirez MA, Yanez-Mo M, Rizos D. Effect of bovine oviductal extracellular vesicles on embryo development and quality in vitro. Reproduction 2017; 153:461–470.

[27] Sohel MM, Hoelker M, Noferesti SS, Salilew-Wondim D, Tholen E, Looft C, Rings F, Uddin MJ, Spencer TE, Schellander K, Tesfaye D. Exosomal and Non-Exosomal Transport of Extra-Cellular microRNAs in Follicular Fluid: Implications for Bovine Oocyte Developmental Competence. PLoS One 2013; 8:e78505.

[28] Frenette G, Lessard C, Madore E, Fortier MA, Sullivan R. Aldose reductase and macrophage migration inhibitory factor are associated with epididymosomes and spermatozoa in the bovine epididymis. Biol Reprod 2003; 69:1586-1592.

[29] Machtinger R, Laurent LC, Baccarelli AA. Extracellular vesicles: roles in gamete maturation, fertilization and embryo implantation. Hum Reprod Update 2016; 22 182-193.

[30] Jamaludin NA, Meikle A, Hunt S, Wachernig H, Thurston LM, Andronowska A, Ebbens S, Fazeli A. Characterisation of extracellular vesicles secreted by oviductal and endometrial epithelial cells. UKEV 2016 Congress, Oxford Brookes University, UK.

[31] Braundmeier AG, Dayger CA, Mehrotra P, Belton RJ Jr, Nowak RA. EMMPRIN is secreted by human uterine epithelial cells in microvesicles and stimulates metalloproteinase production by human uterine fibroblast cells. Reprod Sci 2012; 19:1292-301.

[32] Burnett LA, Light MM, Mehrotra P, Nowak RA. Stimulation of GPR30 increases release of EMMPRIN-containing microvesicles in human uterine epithelial cells. J Clin Endocrinol Metab 2012; 97:4613-22.

[33] Alminana C, Corbin E, Tsikis G, Alcantara-Neto AS, Labas V, Reynaud K, Galio L, Uzbekov R, Garanina AS, Druart X, Mermillod P. Oviduct extracellular vesicles protein content and their role during oviduct-embryo cross-talk. Reproduction 2017; 154 253-268.

[34] Lewis BP, Burge CB, Bartel DP. Conserved seed pairing, often flanked by adenosines, indicates that thousands of human genes are microRNA targets. Cell 2005; 120:15-20.

[35] Fazeli A, Affara NA, Hubank M, Holt WV. Sperm-induced modification of the oviductal gene expression profile after natural insemination in mice. Biology of reproduction 2004; 71:60-5.

[36] Georgiou AS, Snijders AP, Sostaric E. Modulation of the oviductal environment by gametes. Journal of proteome research 2007; 6:4656-66.

[37] Yeste M, Holt WV, Bonet S, Rodriguez-Gil JE, Lloyd RE. Viable and morphologically normal boar spermatozoa alter the expression of heat-shock protein genes in oviductal epithelial cells during co-culture in vitro. Molecular reproduction and development 2014; 81:805-19.

[38] Konstantinidi R, Jamaludin NA, Thurston LM, Hunt S, Fazeli A. Investigating whether the presence of spermatozoa alters the secretion of extracellular vesicles by cultured porcine oviductal epithelial cells in an in vitro model of the female reproductive tract. UKEV 2017 Congress, University of Birmingham, UK.

[39] Miller D, Brinkworth M, Iles D. Paternal DNA packaging in spermatozoa: more than the sum of its parts? DNA, histones, protamines and epigenetics. Reproduction 2010; 139:287-301.

[40] Thery C, Ostrowski M, Segura E. Membrane vesicles as conveyors of immune responses. Nat Rev Immunol 2009; 9:581-593.

[41] Sokolova V, Ludwig AK, Hornung S, Rotan O, Horn PA, Epple M, Giebel B. Characterisation of exosomes derived from human cells by nanoparticle tracking analysis and scanning electron microscopy. Colloids Surf B Biointerfaces 2011; 87:146-150.

[42] Gercel-Taylor C, Atay S, Tullis RH, Kesimer M, Taylor DD. Nanoparticle analysis of circulating cell-derived vesicles in ovarian cancer patients. Anal Biochem 2012; 428:44-53.

[43] Dragovic RA, Gardiner C, Brooks AS, Tannetta DS, Ferguson DJ, Hole P, Carr B, Redman CW, Harris AL, Dobson PJ, Harrison P, Sargent IL. Sizing and phenotyping of cellular vesicles using Nanoparticle Tracking Analysis. Nanomedicine 2011; 7:780-788.

[44] Marimpietri D, Petretto A, Raffaghello L, Pezzolo A, Gagliani C, Tacchetti C, Mauri P, Melioli G, Pistoia V. Proteome profiling of neuroblastoma-derived exosomes reveal the expression of proteins potentially involved in tumor progression. PLoS One 2013; 8:e75054.

[45] Hanaor DA, Ghadiri M, Chrzanowski W, Gan Y. Scalable surface area characterization by electrokinetic analysis of complex anion adsorption. Lanqmuir 2014; 30:15143-52.

[46] Hunter RJ. Zeta potential in colloid science : principles and applications. 1981 London : Academic Press.

[47] Zhang W, Peng P, Kuang Y, Yang J, Cao D, You Y, Shen K. Characterization of exosomes derived from ovarian cancer cells and normal ovarian epithelial cells by nanoparticle tracking analysis. Tumour Biol 2016; 37:4213-21.

[48] Bondar OV, Saifullina DV, Shakhmaeva, II, Mavlyutova, II, Abdullin TI. Monitoring of the Zeta Potential of Human Cells upon Reduction in Their Viability and Interaction with Polymers. Acta Naturae 2012; 4:78-81.

[49] Sathappa M, Alder NN. Ionization Properties of Phospholipids Determined by Zeta Potential Measurements. Bio Protoc 2016; 6:e2030.

[50] Raposo G, Nijman HW, Stoorvogel W, Liejendekker R, Harding CV, Melief CJ, Geuze HJ. B lymphocytes secrete antigen-presenting vesicles. J Exp Med 1996; 183(3):1161-72.

[51] Akers JC, Gonda D, Kim R, Carter BS, Chen CC. Biogenesis of extracellular vesicles (EV): exosomes, microvesicles, retrovirus-like vesicles, and apoptotic bodies. J Neurooncol 2013; 113(1): 1-11.

[52] Blanchard N, Lankar D, Faure F, Regnault A, Dumont C, Raposo G, Hivroz C. TCR activation of human T cells induces the production of exosomes bearing the TCR/CD3/zeta complex. J Immunol 2002; 168(7):3235-41.

[53] André F, Chaput N, Schartz NE, Flament C, Aubert N, Bernard J, Lemonnier F, Raposo G, Escudier B, Hsu DH, Tursz T, Amigorena S, Angevin E, Zitvogel L. Exosomes as potent cell-free peptide-based vaccine. I. Dendritic cell-derived exosomes transfer functional MHC class I/peptide complexes to dendritic cells. J Immunol 2004; 172(4):2126-36.

[54] Simons M, Raposo G. Exosomes - vesicular carriers for intercellular comunication. Curr Opin Cell Biol 2009; 21:575-581.

[55] da Silveira JC, Veeramachaneni DN, Winger QA, Carnevale EM, Bouma GJ. Cell-secreted vesicles in equine ovarian follicular fluid contain miRNAs and proteins: a possible new form of cell communication within the ovarian follicle. Biol Reprod 2012; 86(3):71.

[56] Raposo G, Stoorvogel W. Extracellular vesicles: exosomes, microvesicles, and friends. J Cell Biol 2013; 200:373–383.

[57] Turturici G, Tinnirello R, Sconzo G, Geraci F. Extracellular membrane vesicles as a mechanism of cell-to-cell communication:advantages and disadvantages. Am J Physiol Cell Physiol 2014; 306(7):C621-33.

[58] Aswad H, Jalabert A, Rome S. Depleting extracellular vesicles from fetal bovine serum alters proliferation and differentiation of skeletal muscle cells in vitro. BMC Biotechnol 2016; 16:32.

[59] Jalabert A, Vial G, Guay C, Wiklander OP, Nordin JZ, Aswad H, Forterre A, Meugnier E, Pesenti S, Regazzi R, Danty-Berger E, Ducreux S, Vidal H, El-Andaloussi S, Rieusset J, Rome S. Exosome-like vesicles released from lipid-induced insulin-resistant muscles modulate gene expression and proliferation of beta recipient cells in mice. Diabetologia 2016; 59(5):1049-58.

[60] Piehl LL, Fischman ML, Hellman U, Cisale H, Miranda PV. Boar seminal plasma exosomes: effect on sperm function and protein identification by sequencing. Theriogenology 2013; 79:1071-1082.

[61] Lopera-Vasquez R, Hamdi M, Maillo V, Lloreda V, Coy P, Gutierrez-Adan A, Bermejo-Alvarez P, Rizos D. Effect of bovine oviductal fluid on development and quality of bovine embryos produced in vitro. Reprod Fert Dev. 2015; doi:10.107/RD15238.

[62] Lopera-Vásquez R, Hamdi M, Fernandez-Fuertes B, Maillo V, Beltrán-Breña P, Calle A, Redruello A, López-Martín S, Gutierrez-Adán A, Yañez-Mó M, Ramirez MÁ, Rizos D. Extracellular vesicles from BOEC in in vitro embryo development and quality. PLoS One 2016; 11(2):e0148083.

[63] Miyado K1, Yoshida K, Yamagata K, Sakakibara K, Okabe M, Wang X, Miyamoto K, Akutsu H, Kondo T, Takahashi Y, Ban T, Ito C, Toshimori K, Nakamura A, Ito M, Miyado M, Mekada E, Umezawa A. The fusing ability of sperm is bestowed by CD9-containing vesicles released from eggs in mice. Proc Natl Acad Sci USA 2008; 105:12921–12926.

[64] Saadeldin IM, Oh HJ, Lee BC. Embryonic-maternal cross-talk via exosomes: potential implications. Stem Cells Cloning Adv Appl 2015; 8:103–107.

[65] Burns G, Brooks K, Spencer TE. Extracelluar vesicles originate from the conceptus and uterus during early pregnancy in sheep. Biol Reprod 2016; 94(3):56.

[66] Frenette G, Thabet M, Sullivan R. Polyol pathway in human epididymis and semen. J Androl 2006; 27:233–239.

[67] Frenette G, Girouard J, D'Amours O, Allard N, Tessier L, Sullivan R. Characterization of two distinct populations of epididymosomes collected in the intraluminal compartment of the bovine cauda epididymis. Biol Reprod 2010; 83:473–480.

[68] Belleannee C, Calvo E, Caballero J, Sullivan R. Epididymosomes convey different repertoires of microRNAs throughout the bovine epididymis. Biol Reprod 2013; 89:30.

[69] Ronquist G, Brody I. The prostasome: its secretion and function in man. Biochim Biophys Acta 1985; 822:203–218.

[70] Ronquist GK, Larsson A, Stavreus-Evers A, Ronquist G. Prostasomes are heterogeneous regarding size and appearance but affiliated to one DNA-containing exosome family. Prostate 2012; 72:1736–1745.

[71] Madison MN, Roller RJ, Okeoma CM. Human semen contains exosomes with potent anti-HIV-1 activity. Retrovirology 2014; 11:102.

[72] Santonocito M, Vento M, Guglielmino MR, Battaglia R, Wahlgren J, Ragusa M, Barbagallo D, Borzì P, Rizzari S, Maugeri M, Scollo P, Tatone C, Valadi H, Purrello M, Di Pietro C. Molecular characterization of exosomes and their microRNA cargo in human follicular fluid: bioinformatic analysis reveals that exosomal microRNAs control pathways involved in follicular maturation. Fertil Steril 2014; 102:1751–1761:e1751.

[73] Laulagnier K, Motta C, Hamdi S, Roy S, Fauvelle F, Pageaux JF, Kobayashi T, Salles JP, Perret B, Bonnerot C, Record M. Mast cell- and dendritic cell-derived exosomes display a specific lipid composition and an unusual membrane organization. Biochem J 2004; 380(Pt 1):161-71.

[74] Eldh M, Lötvall J, Malmhäll C, Ekström K. Importance of RNA isolation methods for analysis of exosomal RNA: evaluation of different methods. Mol Immunol 2012; 50(4):278-86.

[75] Smorag L, Zheng Y, Nolte J, Zechner U, Engel W, Pantakani DVK. MicroRNA signature in various cell types of mouse spermatogenesis: Evidence for stage-specifically expressed miRNA-221, -203 and -34b-5p mediated spermatogenesis regulation. Biol Cell 2012; 104:677-692.

[76] Yang F, Wang H, Jiang Z, Chu L, Sun Y, Han J. MicroRNA-19a mediates gastric carcinoma cell proliferation through the activation of nuclear factor-κB. Mol Med Rep 2015; 12:5780-5786.

[77] Ling R, Zhou Y, Zhou L, Dai D, Wu D, Mi L, Mao C, Chen D. Lin28/microRNA-let-7a promotes metastasis under circumstances of hyperactive Wnt signaling in esophageal squamous cell carcinoma. Mol Med Rep 2018; 17: 5265-5271.

[78] Li Y, LIU x, Du A, Zhu X, Yu B. miR-203 accelerates apoptosis and inflammation induced by LPS vai targetting NFIL3 in cardiomyocytes. J Cell Biochem 2018; doi:10.1002/jcb.27955.

[79] Wollenhaupt K, Tomek W, Brüssow KP, Tiemann U, Viergutz T, Schneider F, Nürnberg G. Effects of ovarian steroids and epidermal growth factor (EGF) on expression and bioactivation of specific regulators of transcription and translation in oviductal tissue in pigs. Reproduction 2002; 123(1):87-96.

[80] Wijayagunawardane MP, Hambruch N, Haeger JD, Pfarrer C. Effect of epidermal growth factor (EGF) on the phosphorylation of mitogen-activated protein kinase (MAPK) in the bovine oviduct in vitro: Alteration by heat stress. J Reprod Dev 2015; 61(5):383-9.

[81] Steinberger B, Yu H, Brodmann T, Milovanovic D, Reichart U, Besenfelder U, Artemenko K, Razzazi-Fazeli E, Brem G, Mayrhofer C. Semen modulated secretory activity of oviductal epithelial cells is linked to cellular proteostasis network remodelling: proteomic insights into the early phase of interaction in the oviduct in vivo. J Proteomics 2017; 163:14-27.

[82] Yousef MS, Marey MA, Hambruch N, Hayakawa H, Shimizu T, Hussien HA, Abdel-Razek AK, Pfarrer C, Miyamoto A. Sperm binding to oviduct epithelial cells enhances TGFB1 and IL10

expressions in epithelial cells as well as neutrophils in vitro: prostaglandin E2 as a main regulator od anti-inflammatory response in the bovine oviduct. PLoS One 2016; 11(9):e0162309.

[83] Gantier MP, Stunden HJ, McCoy CE, Behlke MA, Wang D, Kaparakis-Liaskos M, Sarvestani ST, Yang YH, Xu D, Corr SC, Morand EF, Williams BR. A miR-19 regulon that controls NF-KB signalling. Nucleic Acids Res 2012; 40(16):8048-58.

[84] Shelke GV, Lässer C, Gho YS, Lötvall J. Importance of exosome depletion protocols to eliminate functional and RNA-containing extracellular vesicles from fetal bovine serum. J Extracell Vesicles 2014; 3.

[85] Wei Z, Batagov AO, Carter DR, Krichevsky AM. Fetal Bovine Serum RNA Interferes with the Cell Culture derived Extracellular RNA. Sci Rep 2016; 6:31175.

[86] Witwer KW, Buzás EI, Bemis LT, Bora A, Lässer C, Lötvall J, Nolte-'t Hoen EN, Piper MG, Sivaraman S, Skog J, Théry C, Wauben MH, Hochberg F. Standardization of sample collection, isolation and analysis methods in extracellular vesicle research. J Extracell Vesicles 2013; 2.

[87] Eitan E, Zhang S, Witwer KW, Mattson MP. Extracellular vesicle-depleted fetal bovine and human sera have reduced capacity to support cell growth. J Extracell Vesicles 2015; 4:26373.

[88] Gámez-Valero A, Monguió-Tortajada M, Carreras-Planella L, Franquesa Ml, Beyer K, Borràs FE. Size-exclusion chromatography-based isolation minimally alters extracellular vesicles' characteristics comapared to precipitating agents. Sci Rep 2016; 6:33641.

[89] Baranyai T, Herczeg K, Onódi Z, Voszka I, Módos K, Marton N, Nagy G, Mäger I, Wood MJ, El Andaloussi S, Pálinkás Z, Kumar V, Nagy P, Kittel Á, Buzás EI, Ferdinandy P, Giricz Z. Isolation of Exosomes from Blood Plasma: Qualitative and Quantitative Comparison of Ultracentrifugation and Size Exclusion Chromatography Methods. PLoS One 2015; 10(12):e0145686.

[90] Böing AN, van der Pol E, Grootemaat AE, Coumans FA, Sturk A, Nieuwland R. Single-step isolation of extracellular vesicles by size-exclusion chromatography. J Extracell Vesicles 2014; 3.

[91] Thery, C. Isolation and characterization of exosomes from cell culture supernatants and biological fluids. Curr Protoc Cell Biol 2006; Chapter 3:Unit 3.22.

[92] Conde-Vancells J, Rodriguez-Suarez E, Embade N, Gil D, Matthiesen R, Valle M, Elortza F, Lu SC, Mato JM, Falcon-Perez JM. Characterization and comprehensive proteome profiling of exosomes secreted by hepatocytes. J Proteome Res 2008; 7(12):5157-66.

[93] Nordin JZ, Lee Y, Vader P, Mäger I, Johansson HJ, Heusermann W, Wiklander OP, Hällbrink M, Seow Y, Bultema JJ, Gilthorpe J, Davies T, Fairchild PJ, Gabrielsson S, Meisner-Kober NC, Lehtiö J, Smith CI, Wood MJ, El Andaloussi S. Ultrafiltration with size-exclusion liquid chromatography for high yield isolation of extracellular vesicles preserving intact biophysical and functional properties. Nanomedicine: Nanotechnology, Biology and Medicine 2015; 11(4):879-883.

[94] Welton JL, Webber JP, Botos LA, Jones M, Clayton A. Ready-made chromatography columns for extracellular vesicle isolation from plasma. J Extracell Vesicles 2015; 4:27269.

[95] Hurwitz SN, Conlon MM, Rider MA, Brownstein NC, Meckes DG, Jr. Nanoparticle analysis sheds budding insights into genetic drivers of extracellular vesicle biogenesis. J Extracell Vesicles 2016; 5:31295.

[96] Riches A, Campbell E, Borger E, Powis S. Regulation of exosome release from mammary epithelial and breast cancer cells - a new regulatory pathway. Eur J Cancer 2014; 50:1025-1034.

[97] Tian T, Wang Y, Wang H, Zhu Z, Xiao Z. Visualizing of the cellular uptake and intracellular trafficking of exosomes by live-cell microscopy. J Cell Biochem 2010; 111:488-496.

[98] Escrevente C, Keller S, Altevogt P, Costa J. Interaction and uptake of exosomes by ovarian cancer cells. BMC Cancer 2011; 11:108.

[99] Al-Dossary AA, Bathala P, Caplan JL, Martin-DeLeon PA. Oviductosome-sperm membrane interaction in cargo delivery - detection of fusion and underlying molecular players using three-dimensional super-resolution structured illumination microscopy (SR-SIM). Journal of Biological Chemistry 2015; 290 17710-17723.

[100] Han J, Lee Y, Yeom KH, Nam JW, Heo I, Rhee JK, Sohn SY, Cho Y, Zhang BT, Kim VN. Molecular basis for the recognition of primary microRNAs by the Drosha-DGCR8 complex. Cell 2006; 125:887-901.

[101] van der Pol E, Hoekstra AG, Sturk A, Otto C, van Leeuwen TG, Nieuwland R. Optical and non-optical methods for detection and characterization of microparticles and exosomes. J Thromb Haemost 2010; 8:2596-2607.

[102] Wu Y, Deng W, Klinke DJ. Exosomes: improved methods to characterize their morphology, RNA content, and surface protein biomarkers. Analyst 2015; 140:6631-6642.

[103] Akagi T, Kato K, Hanamura N, Kobayashi M, Ichiki T. Evaluation of desialylation effect on zeta potential of extracellular vesicles secreted from human prostate cancer cells by on-chip microcapillary electrophoresis. Japanese Journal of Applied Physics 2014; 53.

[104] Clogston JD, Patri AK. Zeta Potential Measurement. In Characterization of Nanoparticles Intended for Drug Delivery 2011; pp. 63-70.

[105] Veronesi B, de Haar C, Lee L, Oortgiesen M. The surface charge of visible particulate matter predicts biological activation in human bronchial epithelial cells. Toxicology and Applied Pharmacology 2002; 178:144-154.

[106] Altankov G, Richau K, Groth T. The role of surface zeta potential and substratum chemistry for regulation of dermal fibroblasts interaction. Materialwissenschaft Und Werkstofftechnik 2003; 34 1120-1128.

[107] Fontes A, Fernandes HP, Barjas-Castro ML, de Thomaz AA, Pozzo LD, Barbosa LC, Cesar CL. Red blood cell membrane viscoelasticity, agglutination and zeta potential measurements with double optical tweezers - art. no. 608811. Imaging, Manipulation, and Analysis of Biomolecules, Cells, and Tissues IV 2006; 6088 8811-8811

[108] Lin DQ, Zhong LN, Yao SJ. Zeta potential as a diagnostic tool to evaluate the biomass electrostatic adhesion during ion-exchange expanded bed application. Biotechnology and Bioengineering 2006; 95:185-191.

[109] Kato K, Kobayashi M, Hanamura N, Akagi T, Kosaka N, Ochiya T, Ichiki T. Electrokinetic Evaluation of Individual Exosomes by On-Chip Microcapillary Electrophoresis with Laser Dark-Field Microscopy. Japanese Journal of Applied Physics 2013; 52.

[110] Cocucci E, Racchetti G, Meldolesi J. Shedding microvesicles: artefacts no more. Trends Cell Biol 2009; 19:43-51.

[111] Vlassov AV, Magdaleno S, Setterquist R, Conrad R. Exosomes: current knowledge of their composition, biological functions, and diagnostic and therapeutic potentials. Biochim Biophys Acta 2012; 1820:940-948.

[112] Tetta C, Ghigo E, Silengo L, Deregibus MC, Camussi G. Extracellular vesicles as an emerging mechanism of cell-to-cell communication. Endocrine 2013; 44:11-19.

[113] Akagi T, Ichiki T. Cell electrophoresis on a chip: what can we know from the changes in electrophoretic mobility? Anal Bioanal Chem 2008; 391 2433-2441.

[114] Sundelacruz S, Levin M, Kaplan DL. Role of membrane potential in the regulation of cell proliferation and differentiation. Stem Cell Rev 2009; 5:231-246.

[115] Arvizo RR, Miranda OR, Thompson MA, Pabelick CM, Bhattacharya R, Robertson JD, Rotello VM, Prakash YS, Mukherjee P. Effect of nanoparticle surface charge at the plasma membrane and beyond. Nano Lett 2010; 10 2543-2548.

[116] Chang HY, Kao WL, You YW, Chu YH, Chu KJ, Chen PJ, Wu CY, Lee YH, Shyue JJ. Effect of surface potential on epithelial cell adhesion, proliferation and morphology. Colloids Surf B Biointerfaces 2016; 141:179-186.

[117] Walter I. Culture of bovine oviduct epithelial cells (BOEC). Anat Rec 1995; 243:347-356.

Manuscript: Evaluating size exclusion chromatography as a method for the purification of extracellular vesicles secreted by primary and immortalised cells of reproductive origin.

Nurul Akmal Jamaludin et al.*

Highlights:

Reproductive cells secrete distinct populations of extracellular vesicles (EVs)

EVs secreted by reproductive epithelial cells contain microRNAs

The electrokinetic potential of an EV membrane is dependent on its cell of origin

Functionally distinct regions of the oviduct secrete different EVs